Delft University of Technology
Faculty of Electrical Engineering, Mathematics and Computer Science
Delft Institute of Applied Mathematics

Extending the SSVI model with arbitrage-free conditions

A thesis submitted to the
Delft Institute of Applied Mathematics
in partial fulfillment of the requirements

for the degree

MASTER OF SCIENCE
in
APPLIED MATHEMATICS

by

Sebas Hendriks

Delft, the Netherlands
August, 2016

MSc thesis APPLIED MATHEMATICS

"Extending the SSVI model with arbitrage-free conditions"

Sebas Hendriks

Delft University of Technology

Daily supervisor

Dr. C. Martini

Responsible professor

Prof.dr.ir. C.W. Oosterlee

Other thesis comittee member(s)

Dr. C. Kraaikamp

August, 2016

Delft, the Netherlands

Acknowledgements

This thesis has been submitted for the degree Master of Science in Applied Mathematics at Delft University of Technology. The supervisor of this thesis was Kees Oosterlee, professor at the Numerical Analysis group of Delft Institute of Applied Mathematics. Research for this thesis took place during an internship at Zeliade Systems in Paris, under the supervision of Claude Martini.

I would like to thank Claude Martini and everyone else at Zeliade who allowed me to have such a wonderful working experience in such a wonderful city as Paris. Also, I would like to thank Kees Oosterlee for his advice over the course of the project. My thanks also goes out to Thomas van der Zwaard and Jacob de Zoete for their feedback on my draft.

Abstract

This thesis studies the properties and calibration of the SSVI implied volatility surface model. Using previous work done by Gatheral and Jacquier, we derive conditions to guarantee a surface free of static arbitrage. These conditions are then studied more thoroughly. Having shown that there is room for improvement in the model through a calibration on European options, we introduce an extension, eSSVI, which allows for more freedom in the parametrization of the model. Again, conditions to avoid static arbitrage are found and the model is shown to generally provide a superior fit of the European market option data. We then explore the possibility of using SSVI and eSSVI volatility surfaces to be calibrated on American options through the use of local volatility. This is done using Dupire's formula, allowing us to transform implied volatilities to local volatilities. Using the trinomial tree method, we can then derive American option prices allowing us to calibrate a volatility surface on American option data.
Keywords: implied volatility surface, SSVI, local volatility, trinomial tree, American option calibration

Contents

Chapter 1

Introduction

When it comes to financial mathematics, there are often several means to an end. What this means is that there is almost never a fixed method that is universally used and approved. Practically every model is a mere approximation of reality and through the improvement of these models, we attempt to get ever closer to this reality. In this thesis, we will introduce one of these improvements for an implied volatility surface model: SSVI.

The implied volatility surface is a very useful tool for traders and market makers in financial institutions around the globe. In the pricing of options, traders often make use of implied volatilities as a method for seeing whether they think a derivative is under or overpriced. The implied volatility surface allows for an easy comparison of a derivative at different strikes and maturities. Furthermore, it can be used to reduce model risk, as a good estimated volatility surface displays potential instability in the market. Another aspect that is often used is the fact that implied volatilities can be used to price more complex exotic options in numerical schemes, since an analytic evaluation of these prices almost never exists.

The SSVI model, introduced in 2012 by Gatheral and Jacquier [11], has been shown to give a good approximation of the implied volatility surface. However, in order to further develop and increase the quality of this model, this thesis presents an extension of the model.

1.1 Structure of the thesis

An extensive look at all the key financial concepts required to fully understand the remainder of the text is presented in Chapter 2. Since the models discussed in this thesis involve volatility surfaces, the reader is introduced to options, implied volatility and the relation between the Black-Scholes formula and the volatility smile. For those who already posses a sufficient background in financial mathematics, only the last section of the chapter explaining the SSVI model would be considered necessary, since this is the model that we will will look to improve.

In Chapter 3, this SSVI model is calibrated to real market data in an effort to demonstrate its performance in practice. The key here is to ensure that the model is free of any static arbitrage, meaning that we have to give correct bounds to the model parameters. These conditions are already known for a parametric form of the model. If we then look at the model in a non-parametric form, different conditions will hold. In the second half of this chapter we show how to find these new conditions.

In Chapter 4, the new model: eSSVI, as an extension of SSVI is introduced. Here it is assumed that the correlation parameter is non-constant and we examine the implications for the calibration of the model with respect to the same market data. However, before this can be done, we must again be sure that eSSVI does not allow static arbitrage. It turns out, that in order to find these conditions, one must first look at the non-parametric case, which allows us to find the conditions for the parametric case. Having done that, we can actually perform the calibration and compare the results for SSVI and eSSVI.

In Chapter 5, using Dupire's formula, the implied volatility surface found through either SSVI or eSSVI is transformed to local volatilities. Now, using trinomial trees, this can be used to price American options. Whether there is again an improvement in terms of model accuracy when using eSSVI over SSVI is then tested here.

Chapter 6 summarized our conclusions and provides some suggestions for improvements or further future research.

Chapter 2

From Black-Scholes to volatility surfaces

To start off, in this chapter we will look at some of the definitions and formulas that are required in the rest of the thesis. However, it is assumed that the reader already has at least a minimal financial mathematical background. If necessary, the reader is directed to the first chapter of Hull [14].

2.1 Options

At its core, this thesis is a study of options, of which there are many types. The most basic are *European options*, also sometimes referred to as *plain vanilla options*, of which there are two variants: *call* and *put* options. A *European call* option is a contract that gives its holder the right, but not the obligation, to buy an asset at a specified strike price K at some specific time of maturity T. This means that the pay-off of the option at maturity with stock price path S_t can be written as: $[S_T - K]^+ = \max(S_t - K, 0)$.

A *European put* option is a similar contract where for strike K and maturity T the investor has the right, but not the obligation, to sell the asset. For a European put options, the pay-off function is $[K - S_T]^+$.

The *intrinsic value* of a European option is the difference between the strike and the current stock price. Hence, for a European call the intrinsic value at time t is: $S_t - K$, and for a put: $K - S_t$. An option is said to be *in-the-money* (ITM) whenever the intrinsic value is positive, and *out-of-the-money* (OTM) whenever it is negative.

A more complex derivative is the *American option*. This is a contract with strike K and maturity T that gives an investor the right to exercise and receive the intrinsic value at any time $t \leq T$. In essence, an American option is a European option where one has the added choice when to exercise the option.The challenge for financial institutions is to find a good way to price these options. How this works exactly is explained in Chapter 5.

2.2 The Black-Scholes formula

In the option pricing world one of, if not the, most important results is the Black-Scholes formula. Introduced in 1973 by Fischer Black and Myron Scholes [1], an explicit formula for

pricing European options was presented. They started with the dynamics of the price path of an asset S_t, with W_t the Brownian motion under the risk-free measure, as the Geometric Brownian motion:

$$dS_t = rS_t dt + \sigma dW_t. \tag{2.1}$$

Assuming that the return on the riskless asset r and volatility of stock returns σ are constant and that the stock does not pay dividend, the following PDE was found for a pay-off function $V(S_t, t)$:

$$\frac{\partial V}{\partial t} + \frac{1}{2}\sigma^2 S_t^2 \frac{\partial^2 V}{\partial S_t^2} + rS_t \frac{\partial V}{\partial S_t} - rV = 0. \tag{2.2}$$

Using the final condition: $V(S_T, T) = [S_T - K]^+$, the formula for pricing a European call was found to be:

$$C(T, K) = DF_T \left[F_T N(d_1) - N(d_2)K\right], \tag{2.3}$$

with C being the call price, $F_t = S_0 e^{rt}$ the forward price and $DF_t = e^{-rt}$ the discount factor at time t, S_0 the current stock price, T the time of maturity, K the option strike price, r the risk-free rate, σ the volatility of the stock's returns, $N(\cdot)$ the standard normal cdf and:

$$d_1 = \frac{\ln\left(\frac{F_T}{K}\right) + \frac{1}{2}\sigma^2 T}{\sigma\sqrt{T}} \text{ and } d_2 = d_1 - \sigma\sqrt{T}. \tag{2.4}$$

Similarly, the European put option price is given by:

$$P(T, K) = DF_T \left[N(-d_2)K - F_T N(-d_1)\right]. \tag{2.5}$$

These expressions have also led to the phenomenon called the *put-call parity*: $C(T, K) - P(T, K) = DF_T(F_T - K)$, so for a fixed maturity, the difference in call and put prices is linear in K. Note that this equality only holds for European options.

What many praised the formula for is that it shows a direct link between the price of an option and the standard deviation of the stock returns as all other parameters can be estimated explicitly based on market data. Traders would often use this by looking at option prices to see the amount of volatility market makers were expecting.

2.3 Implied volatility smiles

Over the years it has been found that the pricing of European options is not nearly as easy as just using the Black-Scholes formula with parameters obtained from historical market data. The main issue arose after the famous market crash in 1987, as before this time, traders relied more heavily on the formula to price their options. The problem was that the formula assumes market volatility, σ, to be constant and that stock returns log-normal. However, with the high stock price volatility during the crash, traders were vulnerable to high amounts of risk. It is in part due to this event that ever since then the price of options with extreme strike values have been given higher prices and therefore higher values of σ, in order to compensate for this risk.

Since then, the formula was no longer used for pricing, but mainly for quoting option prices in terms of their volatility, which lead to the introduction of the term *implied volatility*. This value was no longer constant, meaning that one of the assumptions of the Black-Scholes formula was no longer true. The volatility has since been written as a function of the strike and the time to maturity:

$$\sigma_{BS}(t, K) : (t, K) \mapsto \sigma_{BS}(t, K). \tag{2.6}$$

When plotted as a function of the strike K, implied volatilities display local maximum for extreme strike prices far from the forward price F_t, resulting in a skew or "smile". It is hence the reason why one would often refer to a volatility smile when one speaks of the implied volatilities for a fixed maturity t. An example of this "smile" effect in the market is given in Figure 2.1 where for a fixed maturity, the implied volatilities of the `S&P 500` are plotted against their strike values, where we find that the forward price $F_t = 1935.35$ for this smile.

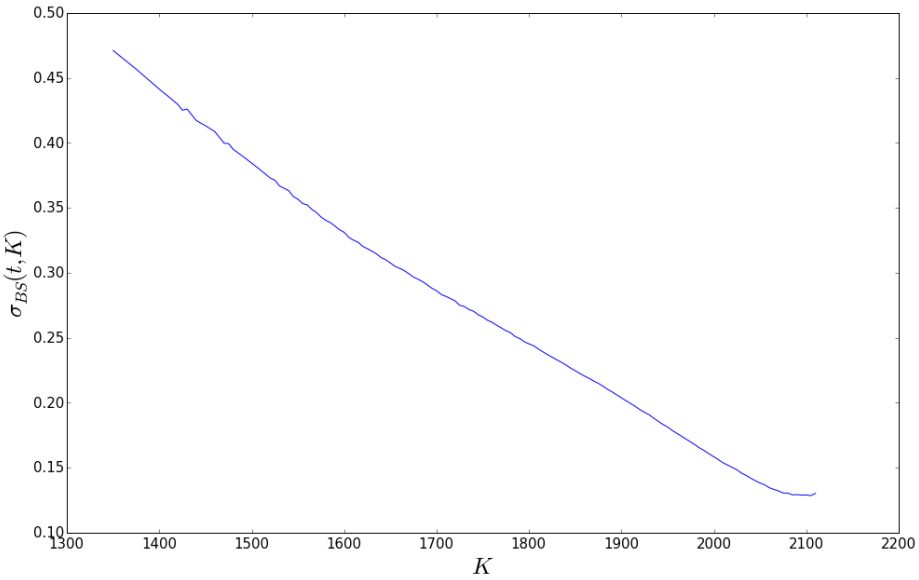

Figure 2.1: Implied volatility smile of S&P 500 data.

It is of critical importance that this is modelled correctly, since the hedging of risk and effectiveness of trading strategies greatly depends on the implied volatility smile. For this purpose, numerous models exist using a varied array of assumptions on the implied volatility. One such assumption is that the volatility is assumed to follow a random process. Some examples are the SABR model by Hagan et al [13] and Gatheral's SVI [9], where it is assumed that this stochastic volatility is a function of a number of parameters that can be calibrated using market data. In this thesis, we will focus on this type of implied volatility.

2.4 Static arbitrage

When a financial model is proposed, proving that it is arbitrage-free is of key importance. The concept of arbitrage, or a "free lunch", is rather simple. If one has a portfolio of cost 0, that has a zero percent probability of becoming a negative value, and a non negative

probability of increasing in value, we speak of an arbitrage opportunity. If at a discrete point in time, arbitrage is possible, this is called *static arbitrage*. Market makers would prefer the market that does not allow these arbitrage opportunities since arbitrageurs could then cut into their profits. For financial engineers, having an arbitrage-free market is also essential, as it is an assumption in most methods for asset pricing.

In [4], the following is concluded concerning arbitrage on volatility surfaces:

Proposition 2.4.1. *A volatility surface is free of static arbitrage if and only if the following conditions are met:*

1. *the surface is free of calendar spread arbitrage;*
2. *each time slice is free of butterfly arbitrage.*

We will now look at both these types of arbitrage.

2.4.1 Calendar spread arbitrage

The calendar spread of option prices is essentially the difference at different maturities in price of options of the same underlying stock at the same moneyness e^k, defined as: $e^k := \frac{K_1}{F_{t_1}} = \frac{K_2}{F_{t_2}}$. For a volatility surface w to be free of calendar spread arbitrage, the following lemma is presented in [11].

Lemma 2.4.2. *A volatility surface w representing the implied total variance: $t\sigma^2_{BS}(k,t)$ is free of calendar spread arbitrage if and only if:*

$$\partial_t w(k,t) \geq 0, \text{ for all } k \in \mathbb{R} \text{ and } t > 0.$$

2.4.2 Butterfly arbitrage

Butterfly arbitrage is essentially the existence of a risk-neutral martingale measure, as described in the first Fundamental Theorem of Asset Pricing by Dybvig and Ross [7]. For a slice of a volatility surface w representing the implied total variance: $t\sigma^2_{BS}(k,t)$ to be butterfly arbitrage-free it requires the corresponding density to be non-negative. Analytically, this means that for the Black-Scholes formula, where we can write: $d_{1,2} = \frac{-k}{\sqrt{w(k)}} \pm \frac{\sqrt{w(k)}}{2}$, and the function $g : \mathbb{R} \to \mathbb{R}$, where:

$$g(k) := \left(1 - \frac{kw'(k)}{2w(k)}\right)^2 - \frac{w'(k)^2}{4}\left(\frac{1}{w(k)} + \frac{1}{4}\right) + \frac{w''(k)}{2}. \tag{2.7}$$

we can now give the following:

Lemma 2.4.3. *A slice is free of butterfly arbitrage if and only if for all $k \in \mathbb{R} : g(k) \geq 0$ and $\lim_{k\to\infty} d_1(k) = -\infty$.*

The proof of both Lemmas 2.4.2 and 2.4.3 can be found in [11]

2.5 Surface Stochastic Volatility Inspired

Numerous models have been developed in an attempt to parametrize the implied volatility smile. A very popular one is the *stochastic volatility implied* or *SVI* parametrization of the implied volatility smile, made public by Gatheral [9] in 2004. One of the reasons for its popularity was that it found that, for a fixed time t, the implied variance $t\sigma_{BS}^2(t,K)$ is linear for extreme strikes K far from the forward price F_t. This follows the moment formula derived by Roger Lee [15]. The modelling of the implied volatility is often done through this implied variance, as it is more stable and therefore easier to parametrize.

There does appear to be a problem with these SVI models as there is increased scepticism that conditions to avoid butterfly arbitrage in this model can be found analytically. Calibration methods are given for several forms of SVI models by Gatheral and Jacquier [11], however these also introduce the parametrically easier Surface SVI, or SSVI model. This SSVI model and the improvements we propose for this model will form the basis of this thesis. We start by looking at some of Gatheral and Jacquier's findings on this SSVI model.

2.5.1 Basics of the SSVI model

The SSVI model gives a transformation of the log-moneyness $k := \log\left(\frac{K}{F_t}\right)$, with K the strike price of the option and F_t the forward price, and the at-the-money (ATM) implied total variance $\theta_t := t\sigma_{BS}^2(0,t)$ to a surface $w(k,t)$ that approximates the implied total variance $t\sigma_{BS}^2(k,t)$. It is assumed that the ATM implied total variance is a function in time of at least class $\mathcal{C}^1$ on $\mathbb{R}_+^*$, and that: $\lim_{t\to 0}\theta_t = 0$. For a smooth function: $\varphi : \mathbb{R}_+^* \to \mathbb{R}_+^*$ such that $\lim_{t\to 0}\theta_t\varphi(\theta_t)$ exists in $\mathbb{R}$, the SSVI parametrization is given by:

$$w(k,\theta_t) = \frac{\theta_t}{2}\left(1 + \rho\varphi(\theta_t)k + \sqrt{(\varphi(\theta_t)k+\rho)^2 + (1-\rho^2)}\right), \tag{2.8}$$

where ρ is a constant with $|\rho| < 1$ representing the correlation between the stock price and its instantaneous volatility. In order to assure that the SSVI surface is free of static arbitrage, two theorems are provided to prove this absence. Here, a condensed versions of the proofs are given.

Theorem 2.5.1 (Theorem 4.1 in [11])**.** *The SSVI surface is free of calendar-spread arbitrage if and only if:*

- $\partial_t\theta_t \geq 0$, *for all* $t \geq 0$*;*
- $0 \leq \partial_\theta(\theta\varphi(\theta)) \leq \frac{1}{\rho^2}\left(1+\sqrt{1-\rho^2}\right)\varphi(\theta)$.

Proof. From Lemma 2.4.2, we saw that, for fixed k, the SSVI surface w is free of calendar spread arbitrage if and only if $\partial_t w(k,\theta_t) = \partial_\theta w(k,\theta_t)\partial_t\theta_t \geq 0$, so it is necessary that both $\partial_t\theta_t$ and $\partial_\theta w(k,\theta_t)$ are positive. For $|\rho| < 1$, we then find that:

$$2\partial_\theta w(k,\theta) = \psi_0(x,\rho) + \gamma(\theta)\psi_1(x,\rho), \tag{2.9}$$

where $x := k\varphi(\theta)$, $\gamma(\theta) := \partial_\theta(\theta\varphi(\theta))/\varphi(\theta)$,

$$\psi_0(x,\rho) := 1 + \frac{1+\rho x}{\sqrt{x^2+2\rho x+1}} \text{ and } \psi_1(x,\rho) := x\left(\frac{x+\rho}{\sqrt{x^2+2\rho x+1}} + \rho\right). \tag{2.10}$$

Through the evaluation of the RHS of (2.9), we find that this equates to:

$$0 \leq \gamma \leq \frac{1+\sqrt{1-\rho^2}}{\rho^2}. \tag{2.11}$$

The result then follows. □

Theorem 2.5.2 (Theorem 4.2 in [11]). *The SSVI surface is free of butterfly arbitrage if for all $\theta > 0$:*

- $\theta\varphi(\theta)(1+|\rho|) < 4$;
- $\theta\varphi^2(\theta)(1+|\rho|) \leq 4$.

Proof. Given Lemma 2.4.3, we start by looking at the function g defined in (2.7) for the SSVI surface w, where we again define: $x := k\varphi(\theta)$:

$$g(x) = \frac{f(x)}{64(x^2+2\rho x+1)^{3/2}}, \tag{2.12}$$

where

$$f(x) := a - b\varphi^2\theta - \frac{c}{16}\varphi^2\theta^2, \tag{2.13}$$

where a, b and c all depend on x. If we now assume that: $0 \leq \theta\varphi(\theta) < \frac{4}{1+|\rho|}$ and $0 \leq \theta\varphi^2(\theta) \leq \frac{4}{1+|\rho|}$, then we can check with the explicit expressions for a, b and c that always $f(x) \geq 0$, thus $g(x) \geq 0$. Also, this first assumption assures that $\lim_{k\to\infty} d_+(k) = -\infty$. □

Some possible functions for φ have been suggested in [11], such as the following power-law representation:

$$\varphi(\theta) := \eta\theta^{-\lambda}. \tag{2.14}$$

Other options are also suggested, but differences in results have been found to be minimal, as is shown in Appendix A. We therefore opt for this simple form for the remainder of the thesis. Here, as we required φ to be a positive function, we need: $\eta > 0$. Now, by using Theorem 2.5.1 we can find conditions on the parameter λ in order to satisfy the calendar spread arbitrage-free conditions. We find for φ as in (2.14) that:

$$\frac{\partial_\theta(\theta\varphi(\theta))}{\varphi(\theta)} = 1-\lambda. \tag{2.15}$$

Since for any $\rho \in (-1,1)$: $\frac{1+\sqrt{1-\rho^2}}{\rho^2} > 1$, if $\lambda \in [0,1]$, it is certain that: $0 \leq 1-\lambda \leq \frac{1+\sqrt{1-\rho^2}}{\rho^2}$, satisfying this condition. Next, by using Theorem 2.5.2 for the butterfly arbitrage-free conditions, it is required that:

$$\begin{cases} \eta\theta^{1-\lambda} < \frac{4}{1+|\rho|}, \\ \eta^2\theta^{1-2\lambda} \leq \frac{4}{1+|\rho|}, \end{cases} \Leftrightarrow \begin{cases} \eta < \frac{4\theta^{\lambda-1}}{1+|\rho|}, \\ \eta \leq \frac{2\theta^{\lambda-1/2}}{\sqrt{1+|\rho|}}, \end{cases} \tag{2.16}$$

Firstly, we see that $\lambda \in [0,1/2]$, as when $\lambda \in (1/2,1]$: $\lim_{\theta\to 0}\theta\varphi^2 \to \infty$. Next, since both functions are increasing functions in θ, for large enough θ the conditions will not hold for a fixed value of η. However, as one in practice only has to deal with $\theta_t \leq \theta_{T_N}$, where T_N is the last maturity given in the market. In this case, we can thus see that we require:

$$0 \leq \eta < \min\left(\frac{4\theta_{T_N}^{\lambda-1}}{1+|\rho|}, \frac{2\theta_{T_N}^{\lambda-1/2}}{\sqrt{1+|\rho}}\right). \tag{2.17}$$

Using this, we can now attempt to calibrate the SSVI model to market data, and evaluate its performance.

Chapter 3

In-depth analysis of the SSVI surface

Having given the conditions for an arbitrage-free SSVI surface, we proceed with calibrating the model parameters on market data. Next, we show that the continuous conditions for calendar spread arbitrage can also be expressed as discrete conditions on the individual surface "slices" corresponding to the maturities given in the market. We observe that the butterfly arbitrage conditions can be enhanced as well through the use of a generalised SSVI formulation. Lastly, we look at how the calibrated model parameters change over time for daily data sets.

3.1 Fitting SSVI to market data

Using the theorems and ideas from [11], we will now look at the steps used to calibrate SSVI to real market data. As mentioned earlier, we will make use of the power-law representation for the function φ, so: $\varphi(\theta_t) = \eta\theta_t^{-\lambda}$. The market option data should supply at least either a set of implied volatilities or mid prices for a set of maturities, $\mathcal{T}$, where for every $t \in \mathcal{T}$ we have a set of strikes: $\mathcal{K}_t$. These mid prices are just the average of the bid and the ask price given by the market, which are used to represent the spot price C_0. If only one of the two sets is provided, the Black-Scholes formula can give us the other. The goal is to find values θ_t and parameters ρ, η and λ such that for every $t \in \mathcal{T}$ and $K \in \mathcal{K}_t$ and $k = \log(K/F_t)$, where the implied total variance given by SSVI, $w(k, \theta_t)$, is converted to a price, $BS(w(k, \theta_t))$, with the smallest possible distance to the market mid price $P(k, t)$.

Note that we compare prices and not implied volatilities, as clearly the accuracy of the prices are of key importance here. Comparison of model and market implied volatilities is inconvenient due to the fact that the derivative of the Black-Scholes price with respect to the implied volatility, the well known *vega*, becomes small for these extreme strike values far from the forward price F_t. This means that for these extreme strikes, the accuracy of the model implied volatility has a very small effect on the accuracy of the implied model prices with respect to the market data.

First, we start by estimating the optimal value for θ_t, which is defined as $t \cdot \sigma_{BS}^2(0, t)$. Therefore, one just needs the value of $\sigma_{BS}(0, t)$ from the data, which is the implied volatility at $K = F_t$, as then $k = \log(F_t/F_t) = 0$. However, since we only know values of σ_{BS} for our given maturities, we can use interpolation to find the value of σ_{BS} at $K = F$.

Next, we calibrate the model, based on SPX data from February 22nd 2016. Having already found θ_t, we focus on the remaining parameters that minimize the distance between the real option prices and the model's option prices, so:

$$\min_{\varphi,\rho} \sum_{t\in\mathcal{T}} \sqrt{\sum_{k\in\mathcal{K}_t} \left(P(k,t) - BS(w(k,\theta_t))\right)^2}. \tag{3.1}$$

Of course, we do this with restrictions on the parameters such that the model is arbitrage-free. From Section 2.5.1 , this corresponds with:

$$\lambda \in [0, 1/2] \text{ and } \eta \leq \min\left(\frac{4\theta_T^{\lambda-1}}{1+|\rho|}, \frac{2\theta_T^{\lambda-1/2}}{\sqrt{1+|\rho|}}\right), \tag{3.2}$$

with T the final maturity given by the market. There are numerous methods available to do this, we used *Sequential Least Squares Programming*-minimizing, as described in [2] to achieve the following results.

For the chosen SPX data set, the values for θ_t are given in Figure 3.1, where they are plotted against their respective maturity t in years. Note that, conforming to the calendar-spread arbitrage condition that $\partial\theta/\partial t \geq 0$ is fulfilled here. Of course, this is to be expected, as these values are derived directly from market data and we can practically ensure that the market data is arbitrage-free. We also see that the values are nearly linear, meaning that the approximate values for θ_t for any $t > 0$ can be found to a high level of accuracy using interpolation methods such as Monotone Piecewise Cubic Interpolation [8].

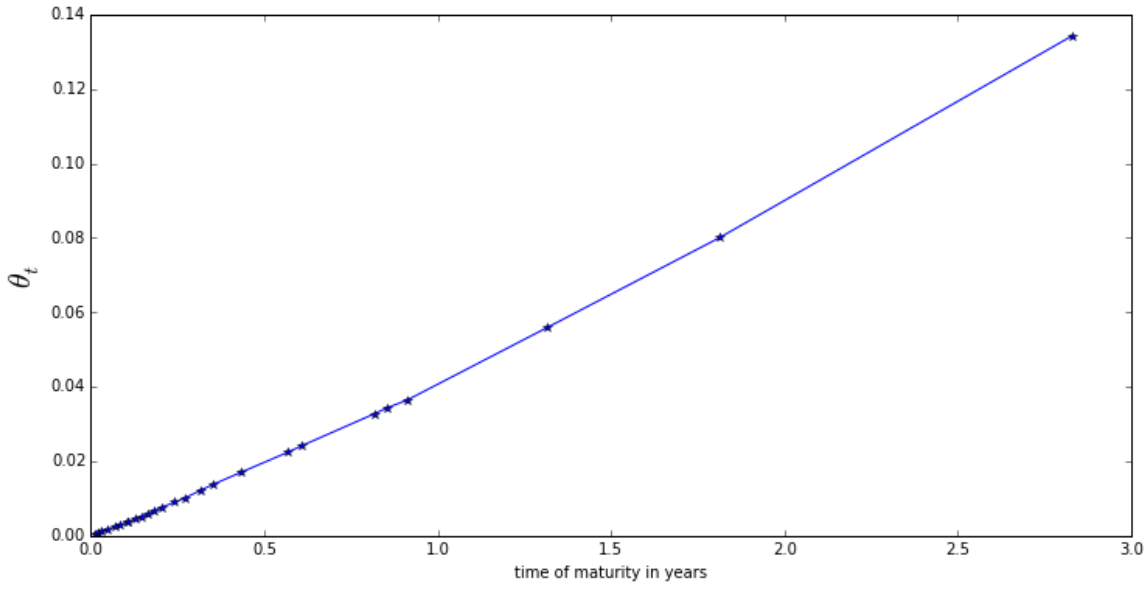

Figure 3.1: Plot of the calibrated values of θ_t.

Having found the values for θ_t, the remaining parameters are estimated using our minimizer as: $\rho = -0.85$, $\eta = 0.93$ and $\lambda = 0.45$. Since the upper bound for η as stated in (3.2) with these values for λ and ρ and $\theta_T = 0.13$ equals: $\eta = 1.63$, it follows that this model is free

of static arbitrage. Hence, we have the function $\varphi(\theta_t) = 0.93\theta_t^{-0.45}$, which we can find in Figure 3.2.

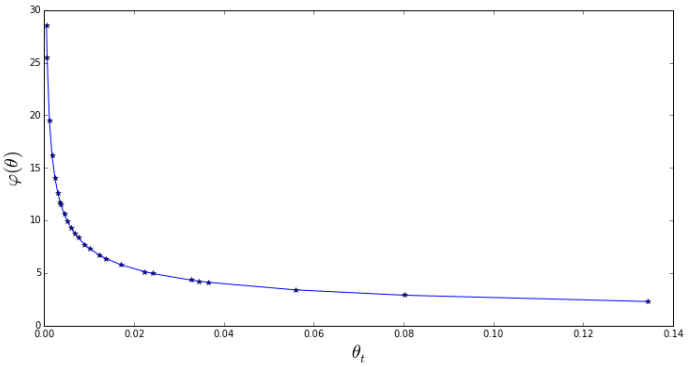

Figure 3.2: Plot of the calibrated values of $\varphi(\theta_t)$.

To demonstrate the quality of the model, the SSVI implied volatility with the bid and ask volatilities of the market for the first, middle and last maturity are given in Figure 3.3. If the model is perfect, the SSVI implied volatility should lie exactly between the bid and ask volatilities. Especially when k is close to zero, as here the influence of the implied volatility is a lot more pronounced on the price, than further away. From Figure 3.3 it can be seen that the fit is generally very good, where only the first maturity appears to be slightly off.

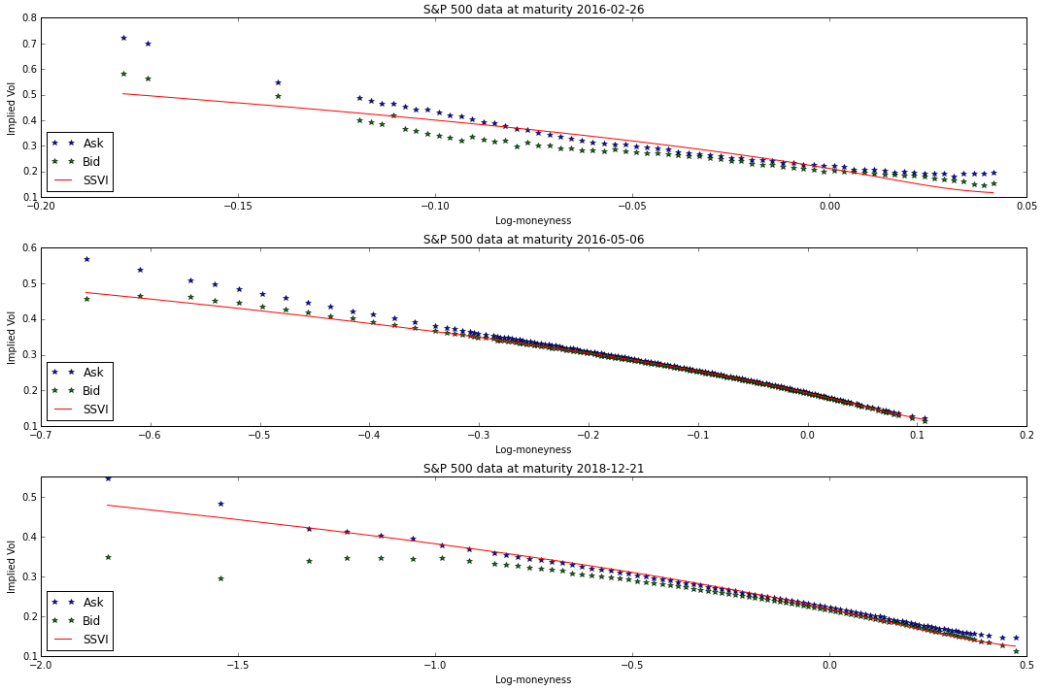

Figure 3.3: Market bid and ask and SSVI volatility smiles for the first, middle and last maturity.

In Table 3.1 we present the average 2-norm distance, D_i, between the model and market price per maturity in bps of the forward price F for the i'th maturity. Naturally,these values should be as small as possible, to indicate a precise calibration. In Table 3.1, we can see that this is indeed the case for all but the last maturity. For this data set, the model is fairly accurate. However, the distances are significantly larger for the first couple of maturities when compared to those near the middle. Hence, we expect that improvements on the model are especially noticeable for the early and late maturities.

i	1	2	3	4	5	6	7	8	9	10	11	12	13
D_i	0.463	0.456	0.392	0.385	0.268	0.268	0.212	0.223	0.168	0.125	0.090	0.070	0.071
i	14	15	16	17	18	19	20	21	22	23	24	25	26
D_i	0.113	0.258	0.172	0.404	0.467	0.497	0.594	0.492	0.533	0.463	0.126	0.758	3.076

Table 3.1: Table of distances of calibrated SSVI model to the data per maturity.

Although the conditions provided by Gatheral and Jacquier [11] to avoid static arbitrage are easy to implement, there are still two aspects that are explored. First, since the market offers a discrete set of maturities, discrete conditions on our parameters can be found such that the model is free of static arbitrage on this discrete set. Second, since it is shown that the butterfly arbitrage conditions are sufficient but not necessary, a general formulation of the SSVI model to find a more accurate butterfly arbitrage condition is used.

3.2 Discrete SSVI arbitrage-free conditions

Due to the fact that the market only has option data for a list of discrete maturities, it may occasionally be practical to have discrete conditions on the model parameters. In such case, we look at the so-called time slices of the SSVI implied volatility surface $w(k, \theta_t)$ for $k \in \mathbb{R}$ and a fixed value t. On these slices, butterfly arbitrage conditions are still the same as before, as they are not time dependent. However, calendar spread arbitrage conditions will change. By definition, it is required that $\partial w/\partial t \geq 0$, which in discrete time means that $w(k, \theta_{t_2}) \geq w(k, \theta_{t_1})$ for all $k \in \mathbb{R}$ and $0 \leq t_1 \leq t_2$.

By definition, a pair of SSVI slices are free of calendar spread arbitrage when, for every $k \in \mathbb{R}$, the slices never cross is. We will look for conditions to ensure this. Define two SSVI slices $w_1 := w(k, \theta_{t_1})$ and $w_2 := w(k, \theta_{t_2})$ where we simplify notation with $\theta_i := \theta_{t_i}$ and $\varphi_i := \varphi(\theta_{t_i})$:

$$w_1 = \frac{\theta_1}{2}(1 + \rho\varphi_1 k + \sqrt{\varphi_1^2 k^2 + 2\rho\varphi_1 k + 1}), \tag{3.3}$$

$$w_2 = \frac{\theta_2}{2}(1 + \rho\varphi_2 k + \sqrt{\varphi_2^2 k^2 + 2\rho\varphi_2 k + 1}). \tag{3.4}$$

Note that the model assumes that the correlation ρ, a fixed value in (-1,1), is identical for the two slices. We now investigate the conditions such that: $w_2 \geq w_1$ for all k, ensuring that the slices never cross, so for all $k \in \mathbb{R}$:

$$\theta_2(1 + \rho\varphi_2 k + \sqrt{\varphi_2^2 k^2 + 2\rho\varphi_2 k + 1}) \geq \theta_1(1 + \rho\varphi_1 k + \sqrt{\varphi_1^2 k^2 + 2\rho\varphi_1 k + 1}). \tag{3.5}$$

For $k = 0$ and $k = \pm\infty$, it is needed that:

$$\begin{cases} \theta_2 \geq \theta_1 & \text{when } k = 0, \\ \theta_2\varphi_2(1+\rho) \geq \theta_1\varphi_1(1+\rho) & \text{when } k = \infty, \\ \theta_2\varphi_2(1-\rho) \geq \theta_1\varphi_1(1-\rho) & \text{when } k = -\infty. \end{cases} \tag{3.6}$$

Since $\rho \in (-1, 1)$, we can simplify (3.6) resulting in:

$$\frac{\theta_2}{\theta_1} \geq 1 \text{ and } \frac{\theta_2\varphi_2}{\theta_1\varphi_1} \geq 1. \tag{3.7}$$

We define: $x := \varphi_1 k$, $\theta := \frac{\theta_2}{\theta_1}$, $\varphi := \frac{\varphi_2}{\varphi_1}$, giving:

$$\theta(1 + \rho\varphi x + \sqrt{\varphi^2 x^2 + 2\rho\varphi x + 1}) \geq (1 + \rho x + \sqrt{x^2 + 2\rho x + 1}), \tag{3.8}$$

and our conditions read: $\theta \geq 1$ and $\theta\varphi \geq 1$. However, when $\theta \geq 1$ and $\theta\varphi = 1$, (3.8) can be simplified to:

$$\theta - 1 + \sqrt{(x + \theta\rho)^2 + \theta^2(1 - \rho^2)} \geq \sqrt{(x + \rho)^2 + 1 - \rho^2}, \tag{3.9}$$

which, since both sides are cleary positive for $\theta \geq 1$ can be squared to find:

$$\sqrt{(x + \theta\rho)^2 + \theta^2(1 - \rho^2)} \geq -(\theta + \rho x). \tag{3.10}$$

When the RHS is negative this always holds, and when it is positive, (3.10) can be squared to find: $x^2 \geq \rho^2 x^2$, which is also always true, meaning the inequality always holds. Therefore the slices never cross and we can be sure that there is no calendar spread arbitrage in this case. In order to evaluate what happens otherwise, we look at (3.8) under the following condition:

$$\theta \geq 1 \text{ and } \theta\varphi > 1. \tag{3.11}$$

3.2.1 Roots of a fourth degree polynomial:

We rewrite (3.8) as: $\alpha + \theta z_2 \geq z_1$ where:

$$\begin{aligned} \alpha &:= \theta(1 + \rho\varphi x) - (1 + \rho x) = \theta - 1 + (\theta\varphi - 1)\rho x, \\ z_1 &:= \sqrt{x^2 + 2\rho x + 1} \text{ and } z_2 := \sqrt{\varphi^2 x^2 + 2\rho\varphi x + 1}. \end{aligned}$$

Note that z_1 and z_2 can be written as: $\sqrt{(x + \rho)^2 + (1 - \rho^2)}$ and $\sqrt{(\varphi x + \rho)^2 + (1 - \rho^2)}$ respectively, which means they are both strictly positive for every $x \in \mathbb{R}$ and $\rho \in (-1, 1)$. Since the function $\alpha + \theta z_2 - z_1$ is continuous, to find conditions such that the inverse of (3.8) is false, one needs to look at the roots of the equality:

$$\alpha + \theta z_2 = z_1. \tag{3.12}$$

Analysing this equality is only possible when we get rid of the square root-terms. Hence, squaring this equation entails $\alpha^2 + 2\alpha\theta z_2 + \theta^2 z_2^2 = z_1^2$, or:

$$2\alpha\theta z_2 = z_1^2 - \alpha^2 - \theta^2 z_2^2. \tag{3.13}$$

Squaring again will entail:

$$P := 4\alpha^2\theta^2 z_2^2 - (z_1^2 - \alpha^2 - \theta^2 z_2^2)^2 = 0. \tag{3.14}$$

Note that if calendar spread is allowed, it is because two slices intersect at a point k^* which is also a root of P. Moreover, due to the intermediate value theorem, the slices will intersect if and only if P has more than one real valued non-zero root. Hence, to ensure the absence of calendar spread arbitrage, we will look at conditions to ensure (3.12) has at most a single real valued non-zero root.

If k^* is a root of P, there are three possibilities:

$$\begin{cases} 2\alpha\theta z_2 = -(z_1^2 - \alpha^2 - \theta^2 z_2^2) & \text{or,} \\ 2\alpha\theta z_2 = z_1^2 - \alpha^2 - \theta^2 z_2^2 \text{ and } \alpha + \theta z_2 = -z_1 & \text{or,} \\ 2\alpha\theta z_2 = z_1^2 - \alpha^2 - \theta^2 z_2^2 \text{ and } \alpha + \theta z_2 = z_1. \end{cases} \tag{3.15}$$

We have seen that only the last case corresponds to an intersection of the slices.

By inserting the values for $\alpha,\ z_1$ and z_2, we find the following expression for P can be found:

$$P(x) = -(\rho^2-1)(\theta\varphi-1)^2(\rho^2(\theta\varphi-1)^2 - (\theta\varphi+1)^2)x^4 + 4\rho\theta(\rho^2-1)(\varphi+1)(\theta\varphi-1)^2x^3 \\ +4\theta(\rho^2-1)(\theta-1)(\theta\varphi^2-1)x^2.$$

However, since $x = \varphi_1 k$ and since we required (3.7) that the smiles do not intersect at $k = 0$, we can drop those roots of P and we are left with a second order polynomial Q with

$$P = x^2 Q. \tag{3.16}$$

3.2.2 Study of the roots of Q

We are examining when there are two real valued roots of equation $Q(x) = 0$ that are also roots of (3.12), where:

$$\begin{aligned} Q(x) \quad = \quad & -(\rho^2-1)(\theta\varphi-1)^2(\rho^2(\theta\varphi-1)^2 - (\theta\varphi+1)^2)x^2 \\ & +4\rho\theta(\rho^2-1)(\varphi+1)(\theta\varphi-1)^2x + 4\theta(\rho^2-1)(\theta-1)(\theta\varphi^2-1). \end{aligned}$$

By setting Q equal to zero, the discriminant is given by:

$$D := 16\theta(\rho-1)^2(\rho+1)^2(\theta\varphi-1)^2(\theta\varphi+1)^2(\rho^2(\theta\varphi-1)^2 - (\theta-1)(\theta\varphi^2-1)). \tag{3.17}$$

Clearly, Q has two real roots if and only if: $(\rho^2(\theta\varphi-1)^2 - (\theta-1)(\theta\varphi^2-1)) > 0$, or:

$$\rho^2 > \frac{(\theta-1)(\theta\varphi^2-1)}{(\theta\varphi-1)^2}. \tag{3.18}$$

This is always possible, since we can show from our conditions in (3.11) that: $\frac{(\theta-1)(\theta\varphi^2-1)}{(\theta\varphi-1)^2} \leq 1$.
If we now define: $Z(x) = z_1^2 - \theta z_2^2 - \alpha^2$, we can see that non-zero roots x_1, x_2 of $Q(x)$ can either be from:

$$2\alpha\theta z_2 = Z(x) \text{ or } 2\alpha\theta z_2 = -Z(x), \tag{3.19}$$

where the roots of the first equation can again be either from:

$$z_1 = \theta z_2 + \alpha \text{ or } -z_1 = \theta z_2 + \alpha. \tag{3.20}$$

It must be noted that, since $\theta z_2 > 0$, we can find out whether $2\alpha\theta z_2 = \pm Z(x)$ by simply checking the signs of α and $Z(x)$. If $Z(x)\alpha < 0$, we know that the found roots of Q are not roots of (3.12). So only when $Z(x)\alpha \geq 0$, we have two real roots for (3.12) when also $\alpha \geq 0$ or $\theta z_2 + \alpha > 0$.

Roots as a function of ρ

Let θ and φ be fixed. Here, we study the situation when Q does have two real roots, which is the case for all ρ such that: $\rho^2 > \frac{(\theta-1)(\theta\varphi^2-1)}{(\theta\varphi-1)^2}$. Let us introduce the notation:

$$\rho^*_\pm := \frac{\pm\sqrt{(\theta-1)(\theta\varphi^2-1)}}{\theta\varphi-1}. \tag{3.21}$$

So we see that Q has roots only when ρ is in the domain $I := (-1, \rho^*_-) \cup (\rho^*_+, 1)$. If we let x_ρ be a root of Q, with ρ in this domain, we can write this as:

$$x_\rho = \frac{2\rho\theta(\varphi+1)}{\rho^2(\theta\varphi-1)^2 - (\theta\varphi+1)^2} \pm \frac{2(\theta\varphi+1)\sqrt{\theta\left(\rho^2(\theta\varphi-1)^2 - (\theta-1)(\theta\varphi^2-1)\right)}}{(\theta\varphi-1)\left(\rho^2(\theta\varphi-1)^2 - (\theta\varphi+1)^2\right)}. \tag{3.22}$$

Using this value of x_ρ, explicit expressions for α and Z can be found, namely $\alpha(x_\rho)$ and $Z(x_\rho)$. We see that they are all continuous functions of ρ, since $(\theta\varphi - 1) > 0$ and $\rho^2(\theta\varphi - 1)^2 - (\theta\varphi+1)^2 < 0$.

Lemma 3.2.1. *$\rho \to \alpha(x_\rho)Z(x_\rho)$ does not change sign for $\rho \in (-1, 1)$.*

Proof. Assume the opposite, so there is a change of sign, then necessarily: $\alpha(x_\rho)Z(x_\rho) = 0$ for some $\rho \in (-1, 1)$. Since we have that: $2\alpha\theta z_2 = \pm Z$, we see that $Z(x_\rho) = 0 \Leftrightarrow \alpha(x_\rho) = 0$, so if $\alpha(x_\rho) = Z(x_\rho) = 0$, we get:

$$\begin{aligned}
&\begin{cases} z_1^2 - \theta^2 z_2^2 = 0 \\ \theta(1+\rho\varphi x) = 1 + \rho x \end{cases} && \Rightarrow \quad \begin{cases} \theta^2(\varphi^2x^2 + 2\rho\varphi x + 1) = x^2 + 2\rho x + 1 \\ \theta^2(\rho^2\varphi^2x^2 + 2\rho\varphi x + 1) = \rho^2x^2 + 2\rho x + 1 \end{cases} \\
&&& \Rightarrow \quad (1-\rho^2)\theta^2\varphi^2x^2 = (1-\rho^2)x^2 \qquad \text{(subtracting the two equations)} \\
&&& \Leftrightarrow \quad \theta^2\varphi^2 = 1.
\end{aligned}$$

which contradicts (3.11). □

Lemma 3.2.2. *For ρ^* as defined in (3.21), $\alpha(x_{\rho^*_\pm})Z(x_{\rho^*_\pm}) < 0 \Leftrightarrow 0 < \varphi < 1$.*

Proof. Indeed by a direct computation:

$$x_{\rho^*_\pm} = \frac{2\rho^*_\pm\theta(\varphi+1)}{{\rho^*_\pm}^2(\theta\varphi-1)^2 - (\theta\varphi+1)^2} = \mp\frac{2\sqrt{(\theta-1)(\theta\varphi^2-1)}}{(\varphi+1)(\theta\varphi-1)}, \tag{3.23}$$

and

$$\alpha(x_{\rho^*_\pm})Z(x_{\rho^*_\pm}) = \frac{2\theta(\theta-1)^2(\varphi-1)^3(\theta\varphi+1)^3}{(\varphi+1)^3(\theta\varphi-1)^3}, \tag{3.24}$$

and the result follows. □

Combining Lemma 3.2.1 and Lemma 3.2.2 one can show that we have $\alpha(x_\rho)Z(x_\rho) < 0$ if and only if $0 < \varphi < 1$, meaning that under our (3.7) we have no crossing slices when $\varphi < 1$.

Conversely, we can show that if $\varphi > 1$ and $\rho^2 > \frac{(\theta-1)(\theta\varphi^2-1)}{(\theta\varphi+1)^2}$, we have that the two roots of Q are also roots of (3.12).

Lemma 3.2.3. *If $\varphi > 1$, then $\alpha(x_{\rho^*_\pm}) < 0$ and $\alpha + \theta z_2 > 0$.*

Proof. First:

$$\alpha(x_{\rho^*_\pm}) = -\frac{(\theta-1)(\varphi-1)(\theta\varphi+1)}{(\varphi+1)(\theta\varphi-1)} < 0. \tag{3.25}$$

Next, we need to show that $\alpha + \theta z_2$ does not change signs for any value of ρ in the domain I. If the opposite were true, then there would exist a ρ^* such that for roots x_{ρ^*} of Q we have that: $\alpha(x_{\rho^*}) + \theta z_2(x_{\rho^*}) = 0$. However, since $\alpha + \theta z_2 = \pm z_1$, also $z_1(x_{\rho^*}) = 0$, which is not possible for $\rho \in (-1, 1)$. Now, if we evaluate at $x_{\rho^*_\pm}$, we get that for $\alpha(x_{\rho^*_\pm}) + \theta z_2(x_{\rho^*_\pm})$:

$$\begin{aligned} \alpha(x_{\rho^*_\pm}) + \theta z_2(x_{\rho^*_\pm}) &= \frac{(\theta\varphi+1)(\theta|\varphi-1| - \theta(\varphi-1) + \varphi - 1)}{(\varphi+1)(\theta\varphi-1)} \\ &= \frac{(\theta\varphi+1)(\varphi-1)}{(\varphi+1)(\theta\varphi-1)} > 0 \quad \text{when } \varphi > 1. \end{aligned}$$

From this, the result follows. □

We can summarize the cases when roots of Q are also roots of (3.12) and therefore the slices cross with the following proposition:

Proposition 3.2.4. *Assume $\theta \geq 1$ and $\theta\varphi > 1$. Then the slices intersect if and only if:*

$$\varphi > 1 \text{ and } \rho^2 > \frac{(\theta-1)(\theta\varphi^2-1)}{(\theta\varphi-1)^2}. \tag{3.26}$$

3.2.3 SSVI discrete calendar spread conditions

First of all, the necessary conditions: $\theta \geq 1$ and $\theta\varphi \geq 1$, must always hold to allow $w_2 \geq w_1$. Next, to ensure that the slices do not cross, it is required that:

- $\varphi \leq 1$, or
- $\rho^2 \leq \frac{(\theta-1)(\theta\varphi^2-1)}{(\theta\varphi-1)^2}$.

3.3 Graphical illustration

Here, a quick illustration of these conditions is given. Naturally, one needs to ensure that the necessary conditions of (3.11) hold. We give four figures of pairs of SSVI slices in Figure 3.4.

Figure 3.4 (a) displays SSVI slices that intersect, since we here have: $\theta = \varphi = 2$ and $\rho = -\sqrt{\frac{8}{9}}$. This means that we have $\theta > 1$, $\theta\varphi > 1$ and $\varphi > 1$. Therefore since:

$$\frac{(\theta-1)(\theta\varphi^2-1)}{(\theta\varphi-1)^2} = \frac{1\cdot 7}{9} \Rightarrow \rho^2 > \frac{7}{9}, \tag{3.27}$$

in accordance with Proposition 3.2.4, the two slices intersect.

For Figure 3.4 (b) we have that :$\theta = \varphi = 2$ and $\rho = -\sqrt{\frac{7}{9}}$. This means that $\varphi > 1$ and $\rho^2 = \frac{(\theta-1)(\theta\varphi^2-1)}{(\theta\varphi-1)^2}$. Proposition 3.2.4 now dictates that the slices touch but do not cross, which the figure confirms.

For Figure 3.4 (c) and 3.4 (d) we now take: $\theta = \varphi = 2$ and $\rho = -\sqrt{\frac{6}{9}}$, and $\theta = 3$, $\varphi = 0.5$ and $\rho = -0.5$ respectively. In the first case we have that $\varphi > 1$, but $\rho^2 < \frac{(\theta-1)(\theta\varphi^2-1)}{(\theta\varphi-1)^2}$. In the second $\varphi < 1$ and $\rho^2 > \frac{(\theta-1)(\theta\varphi^2-1)}{(\theta\varphi-1)^2}$. Here, Proposition 3.2.4 says that both cases should have pairs of SSVI smiles that do not intersect, and this is shown to be true in the figure.

From Figure 3.4 it can be seen that plots follow our expectations. The smiles only intersect in the case where we expect them to, otherwise they do not.

3.4 Finding continuous conditions

Here, what happens when the time differences between the two SSVI slices and so also between θ_1 and θ_2 are infinitesimally small is examined. This means that: $d\theta = \theta_2 - \theta_1 \Rightarrow \theta_2 = \theta_1 + d\theta$ with $d\theta \to 0$. Hence, in this case, if we call $\theta = \theta_1$, we get: $\frac{\theta_2}{\theta_1} = 1 + \frac{d\theta}{\theta}$. Likewise, since the function φ is dependent on θ_t, we get that: $\varphi\prime(\theta)d\theta = \varphi_2 - \varphi_1 \Rightarrow \varphi_2 = \varphi_1 + \varphi\prime(\theta)d\theta$, so if again $\varphi = \varphi_1$, we have: $\frac{\varphi_2}{\varphi_1} = 1 + \frac{\varphi\prime(\theta)d\theta}{\varphi}$.

We define: $\gamma := \frac{1}{\varphi}\frac{d(\theta\varphi)}{d\theta} = 1 + \theta\frac{\varphi\prime(\theta)}{\varphi}$. If we now fill these values into the previously found conditions we can derive conditions on these new parameters. We should find back the necessary and sufficient condition of Gatheral and Jacquier for the absence of calendar spread arbitrage as given in Theorem 2.5.1.

3.4.1 Necessary conditions

The necessary condition regulates that: $\frac{\theta_2}{\theta_1} \geq 1$. If we take an infinitesimal distance between θ_1 and θ_2, this is equivalent to:

$$\frac{\theta_2}{\theta_1} = 1 + \frac{d\theta}{\theta} \geq 1 \Leftrightarrow \frac{d\theta}{\theta} \geq 0 \Leftrightarrow \frac{d\theta}{dt} \geq 0. \tag{3.28}$$

Note that with $d\theta \to 0$, we can assume $\mathcal{O}(d\theta^2) \approx 0$. Now, for our second necessary condition: $\theta\varphi \geq 1$, in infinitesimal form, this amounts to:

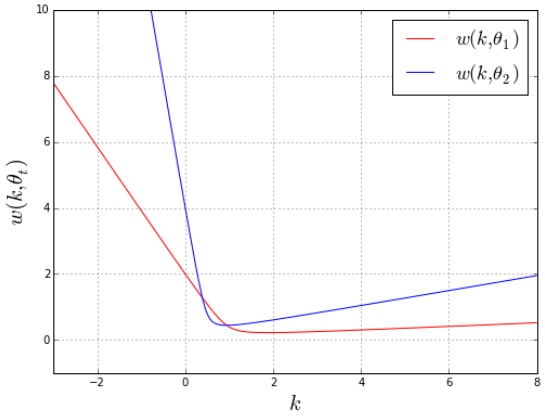

(a) Case where the SSVI smiles intersect.

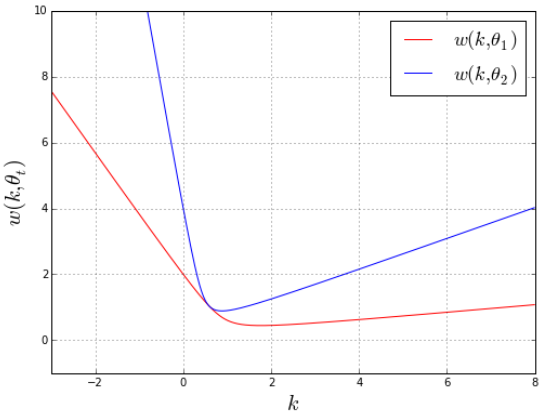

(b) Case where the SSVI smiles touch, but do not intersect.

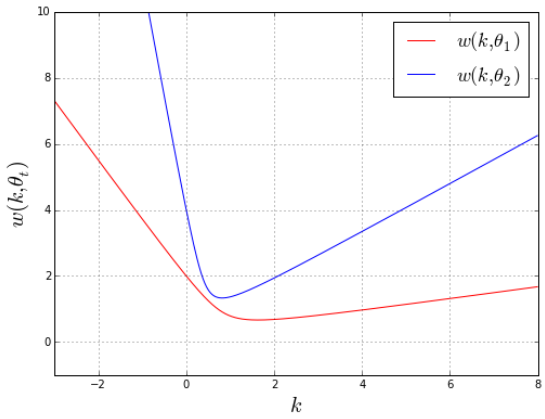

(c) Case where the SSVI smiles never intersect.

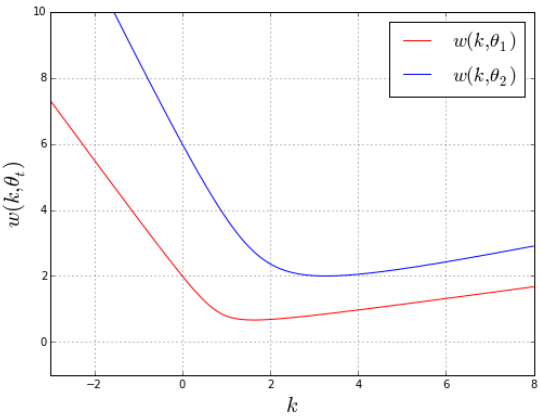

(d) Case where the SSVI smiles never intersect.

Figure 3.4: Various pairs of SSVI slices.

$$\begin{aligned}\left(1+\frac{d\theta}{\theta}\right)\left(1+\frac{\varphi\prime(\theta)}{\varphi}d\theta\right) \geq 1 \Leftrightarrow 1+\left(\frac{1}{\theta}+\frac{\varphi\prime(\theta)}{\varphi}\right)d\theta+\mathcal{O}(d\theta^2) &\geq 1\\ \Leftrightarrow \left(\frac{1}{\theta}+\frac{\varphi\prime(\theta)}{\varphi}\right)d\theta &\geq 0\\ \Leftrightarrow 1+\theta\frac{\varphi\prime(\theta)}{\varphi} &\geq 0 \Leftrightarrow \gamma \geq 0.\end{aligned}$$

For infinitesimal time difference these conditions give us: $\partial\theta/\partial t \geq 0$ and $\gamma \geq 0$.

3.4.2 Secondary conditions

Besides these necessary conditions, we saw that the slices did not cross if either: $\varphi \leq 1$ or $\rho \leq \frac{(\theta-1)(\theta\varphi^2-1)}{(\theta\varphi-1)^2}$. So in the infinitesimal case we get:

$$\begin{aligned} 1 + \frac{\varphi\prime(\theta)}{\varphi} d\theta \leq 1 \quad &\Leftrightarrow \quad \frac{\varphi\prime(\theta)}{\varphi} \geq 0 \\ &\Leftrightarrow \quad 1 + \theta \frac{\varphi\prime(\theta)}{\varphi} \geq 1 \\ &\Leftrightarrow \quad \gamma \geq 1. \end{aligned}$$

Next, for our expressions of θ and φ we see that:

$$\begin{aligned} (\theta\varphi - 1)^2 &= ((1 + \frac{d\theta}{\theta})(1 + \frac{\varphi\prime(\theta)}{\varphi(\theta)} d\theta) - 1)^2 = \left(\frac{d\theta}{\theta}\right)^2 \left(1 + \theta \frac{\varphi\prime(\theta)}{\varphi(\theta)}\right)^2 + \mathcal{O}(d\theta^4) \\ (\theta - 1)(\theta\varphi^2 - 1) &= \frac{d\theta}{\theta} \left(\left(1 + \frac{d\theta}{\theta}\right) \left(1 + \frac{\varphi\prime(\theta)}{\varphi(\theta)} d\theta\right)^2 - 1 \right) = \left(\frac{d\theta}{\theta}\right)^2 \left(1 + 2\theta \frac{\varphi\prime(\theta)}{\varphi(\theta)}\right) + \mathcal{O}(d\theta^2). \end{aligned}$$

Eliminating all higher order terms of $d\theta$, this simplifies to:

$$\rho^2 \left(1 + \theta \frac{\varphi\prime(\theta)}{\varphi(\theta)}\right)^2 \left(\frac{d\theta}{\theta}\right)^2 \leq \left(1 + 2\theta \frac{\varphi\prime(\theta)}{\varphi(\theta)}\right) \left(\frac{d\theta}{\theta}\right)^2,$$

where, if we now cancel out the $(d\theta/\theta)^2$ terms and insert γ into our equation, we get:

$$\rho^2\gamma^2 \leq 2\gamma - 1 \Leftrightarrow \rho^2\gamma^2 - 2\gamma + 1 \leq 0, \tag{3.29}$$

which is only true if γ lies between the roots of this polynomial:

$$\gamma_{1,2} = \frac{2 \pm \sqrt{4 - 4\rho^2}}{2\rho^2} = \frac{1 \pm \sqrt{1 - \rho^2}}{\rho^2}, \tag{3.30}$$

which gives: $\frac{1-\sqrt{1-\rho^2}}{\rho^2} \leq \gamma \leq \frac{1+\sqrt{1-\rho^2}}{\rho^2}$.

3.4.3 SSVI continuous calendar spread conditions

The necessary conditions resulted in: $\frac{d\theta}{dt} \geq 0$ and $\gamma \geq 0$. If we combine this with the fact that we need either $\gamma \leq 1$, or $\frac{1-\sqrt{1-\rho^2}}{\rho^2} \leq \gamma \leq \frac{1+\sqrt{1-\rho^2}}{\rho^2}$, where since $\frac{1}{2} \leq \frac{1-\sqrt{1-\rho^2}}{\rho^2} \leq 1$ and $1 \leq \frac{1+\sqrt{1-\rho^2}}{\rho^2}$ for all possible values of ρ, we have that our final conditions are:

- $\frac{d\theta}{dt} \geq 0$
- $0 \leq \gamma \leq \frac{1+\sqrt{1-\rho^2}}{\rho^2}$

which are also exactly the Gatheral and Jacquier necessary and sufficient conditions for absence of arbitrage stated in Theorem 2.5.1.

3.5 Generalised SSVI butterfly arbitrage conditions

As stated in Theorem 2.5.2, conditions to prevent butterfly arbitrage were given, which we can transform to what we will call the Gatheral and Jacquier bounds:

$$\begin{cases} \theta\varphi(\theta)^2 < \frac{4}{1+|\rho|} & \text{if } \theta \leq \frac{4}{1+|\rho|}, \\ \theta\varphi(\theta)^2 \leq \frac{16}{\theta(1+|\rho|)^2} & \text{if } \theta \geq \frac{4}{1+|\rho|}. \end{cases} \tag{3.31}$$

However, from the proof of Theorem 2.5.2 it is clear that this bound is merely sufficient to prevent arbitrage, but not necessary. To deal with this, a more general formulation of the SSVI model was examined in [12]. Here, they consider an implied volatility surface using the following parametrization:

$$w(k,t) = \theta_t \Psi(k\varphi(\theta_t)), \text{ for all } k \in \mathbb{R}, \ t \geq 0, \tag{3.32}$$

where Ψ is a non-constant, twice differentiable function in $\mathbb{R}$ with $\Psi(0) = 1$ such that:

$$\lim_{k\to\infty} \frac{-k}{\sqrt{w(k,t)}} + \frac{1}{2}\sqrt{w(k,t)} = -\infty. \tag{3.33}$$

If we define $z := k\varphi(\theta_t)$, this function $\Psi(z)$ in the SSVI case is given by:

$$\Psi(z) := \frac{1}{2}\left(1 + \rho z + \sqrt{z^2 + 2\rho z + 1}\right). \tag{3.34}$$

Now, for $\theta > 0$ the following set is defined:

$$\mathcal{Z}_+(\theta) := \left\{ z \in \mathbb{R} : 4\left(\frac{\Psi'(z)^2}{\Psi(z)} - 2\Psi''(z)\right) + \theta\Psi'(z)^2 > 0 \right\}, \tag{3.35}$$

together with the function $\Lambda : (0, \theta_\infty] \times \mathbb{R} \to \mathbb{R} \cup \{+\infty\}$, where:

$$\Lambda(\theta, z) := 16\left(1 - \frac{z\Psi'(z)}{2\Psi(z)}\right)^2 \left(4\left(\frac{\Psi'(z)^2}{\Psi(z)} - 2\Psi''(z)\right) + \theta\Psi'(z)^2\right)^{-1}. \tag{3.36}$$

From this, the following is proposed:

Proposition 3.5.1 (Proposition 4.1 in [12])**.** *The surface w given in (3.32) is free of butterfly arbitrage if and only if:*

$$\theta\varphi(\theta)^2 \leq \inf_{z\in\mathcal{Z}_+(\theta)} \Lambda(\theta, z), \quad \textit{for all } \theta > 0). \tag{3.37}$$

The proof of this proposition follows from the fact that one just needs to show that the function $g(k)$ given in (2.7) is always positive, as from the definition of Ψ it is known that: $\lim_{k\to\infty} d_1 = -\infty$. Filling in the new general function for w from (3.32) gives us the result.

Unfortunately, when we use the SSVI form for $\Psi(z)$, only an analytic solution to (3.37) exists when $\rho = 0$ or $\rho = \pm 1$. When this is not the case, this solution need to be approximated numerically. For $\rho = 0$, the following result is given:

$$\theta\varphi(\theta)^2 \leq A^*(\theta)\mathbf{1}_{\{\theta<4\}} + \frac{16}{\theta} \cdot \mathbf{1}_{\{\theta\geq 4\}}, \tag{3.38}$$

where:

$$A^*(\theta) = \frac{16y(y+1)}{8(y-2) + \theta y(y-1)}, \text{ with } y = \frac{2}{1-\theta/4} + \sqrt{\left(\frac{2}{1-\theta/4}\right)^2 + \frac{2}{1-\theta/4}}. \tag{3.39}$$

3.5.1 Uncorrelated SSVI

Here, the difference between the SSVI and the generalised butterfly arbitrage bound when $\rho = 0$ is examined. From (3.31) and (3.38) it can be seen that for $\theta \geq 4$, the conditions are identical, except that the generalised version allows $\theta\varphi(\theta)^2 = 16/\theta$. However, it can also be shown using, the value of $A^*(\theta)$, that the generalised boundary is strictly greater than the Gatheral and Jacquier boundary for $\theta < 4$.

Lemma 3.5.2. *For all* $0 \leq \theta < 4$: $A^*(\theta) > 4$.

Proof. We need to show that for every $0 \leq \theta < 4$: $\frac{16y(y+1)}{8(y-2)+\theta y(y-1)} > 4$, with $y = \frac{8+\sqrt{8(12-\theta)}}{4-\theta}$. This is equivalent to:

$$\begin{aligned}
\frac{4y(y+1)}{8(y-2)+\theta y(y-1)} > 1 \quad &\Leftrightarrow \quad (4-\theta)y^2 - (4-\theta)y + 16 > 0 \\
&\Leftrightarrow \quad \frac{160 - 8\theta + 16\sqrt{96-8\theta}}{4-\theta} + 8 - \sqrt{96-8\theta} > 0 \\
&\Leftrightarrow \quad \frac{16(12-\theta) + (12+\theta)\sqrt{8(12-\theta)}}{4-\theta} > 0,
\end{aligned}$$

which is clearly true for all $0 \leq \theta < 4$. □

Graphically, we can also check whether this is true, as seen in Figure 3.5. Here, it can be seen that there is a significant difference between the respective upper bounds for the value of $\theta\varphi(\theta)^2$. This would mean that in some cases a calibration might limit the parameters of φ in order to satisfy the conditions of Theorem 2.5.2, where this would in fact not be necessary to prevent butterfly arbitrage. Now, we will examine the value of the the generalised bound when $\rho \neq 0$.

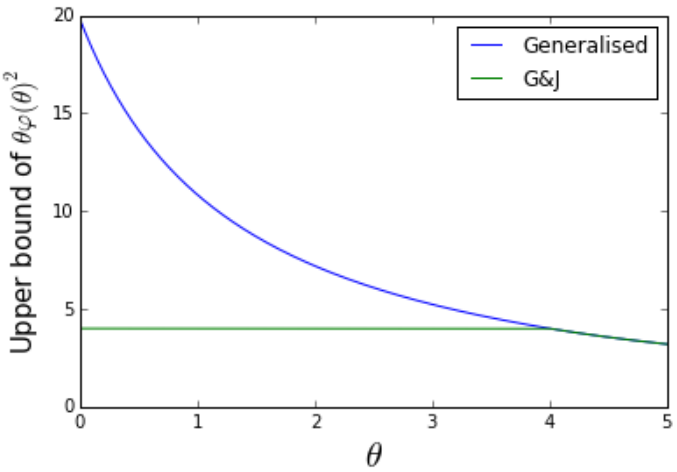

Figure 3.5: Comparison of the generalised and Gatheral and Jacquier bound of $\theta\varphi(\theta)^2$.

3.5.2 Correlated SSVI

Unfortunately, there is no analytic expression for the generalised bound on our parameters to avoid butterfly arbitrage of SSVI. The only way to find this bound is through numerical

methods, meaning that the computational time is greatly increased. However, one can, just as in the uncorrelated case, show that the generalised bound is always less strict for any value of ρ.

First off, we start by looking when $\theta \geq \frac{4}{1+|\rho|}$. From (3.31), the Gatheral and Jacquier bound is: $\theta\varphi(\theta)^2 < \frac{16}{\theta(1+|\rho|)^2}$. According to the generalised formulation, it is needed that:

$$\theta\varphi(\theta)^2 \leq \inf_{z\in\mathcal{Z}_+(\theta)} \Lambda(z,\theta) = \inf_{z\in\mathcal{Z}_+(\theta)} \frac{16a(z)}{4b(z)+\theta c(z)}, \tag{3.40}$$

where:

$$a(z) = \frac{1}{4}\left(1+\frac{1}{y}\right)^2,\ b(z) = \frac{y^2+(2\rho^2+\rho z-1)y-2(1-\rho^2)}{2y^3} \text{ and } c(z) = \frac{(z+\rho+\rho y)^2}{4y^2}, \tag{3.41}$$

with $y := \sqrt{z^2+\rho z+1}$ and $z := k\varphi(\theta)$. So, when $\theta \geq \frac{4}{1+|\rho|}$ the derivative of $\Lambda(z,\theta)$ with respect to z is always negative for all $z \in \mathcal{Z}_+(\theta)$ if $\rho \geq 0$ and always positive when $\rho < 0$. This means that the infimum of our interest lies at $z \to \pm(\rho)\infty$, depending on the sign of ρ. Using the values above it can be shown:

$$\begin{aligned}\lim_{z\to\text{sgn}(\rho)\infty} \Lambda(z,\theta) &= \lim_{z\to\text{sgn}(\rho)\infty} \frac{16y(y+1)^2}{8y^2+8(2\rho^2+\rho z-1)y-16(1-\rho^2)+\theta y(z+\rho+\rho y)^2} \\ &= \frac{16}{\theta(1+|\rho|)^2}.\end{aligned}$$

Hence, for high values of θ, the generalised conditions are practically identical to the Gatheral and Jacquier bound except for the inequality.

Next we show that the bound for $\theta\varphi(\theta)^2$ for fixed ρ and z is strictly decreasing in θ. First note that the set $Z_+(u)$ increases in size as u becomes larger. This is due to the fact that, if $b(z)$ is positive for a given value of z, $z \in Z_+(u)$ for all values of u. However, if $b(z)$ is negative, only for $u \geq \frac{-4b(z)}{c(z)}$ will $z \in Z_+(u)$. From this we see that the set is increasing in size for larger u.

Now, for fixed z, $\Lambda(\theta,z)$ is strictly decreasing for increasing values of θ, as $c(z)$ is always positive. This means that for θ_1, θ_2 with $\theta_2 > \theta_1$:

$$\forall z \in \mathbb{R}:\ \Lambda(\theta_2,z) < \Lambda(\theta_1,z) \Rightarrow \inf_{z\in Z_+(\theta_1)} \Lambda(\theta_2,z) < \inf_{z\in Z_+(\theta_1)} \Lambda(\theta_1,z). \tag{3.42}$$

However, since $Z_+(\theta)$ is a set that increases in size with θ, $\inf_{z\in Z_+(\theta_2)} \Lambda(\theta_2,z) < \inf_{z\in Z_+(\theta_1)} \Lambda(\theta_2,z)$.

From this it follows that: $\inf_{z\in Z_+(\theta_2)} \Lambda(\theta_2,z) < \inf_{z\in Z_+(\theta_1)} \Lambda(\theta_1,z)$, meaning that indeed our upper bound decreases in θ for fixed ρ and z.

Combining the fact that the value of $\inf_{z\in Z_+(\theta)} \Lambda(z,\theta)$ is strictly decreasing in θ and that the bound for $\theta \geq \frac{4}{1+|\rho|}$ equals $\inf_{z\in Z_+(\theta)} \Lambda(z,\theta) = \frac{16}{\theta(1+|\rho|)^2}$, we can state that for $\theta < \frac{4}{1+|\rho|}$, the generalised upper bound of $\theta\varphi(\theta)^2$ is:

$$\inf_{z\in Z_+(\theta)} \Lambda(z,\theta) > \inf_{z\in Z_+(\frac{4}{1+|\rho|})} \Lambda(z, \frac{4}{1+|\rho|}) = \frac{4}{1+|\rho|}. \tag{3.43}$$

However, since the original bound was given as $\frac{4}{1+|\rho|}$, it is certain that the generalised bound is always greater than the Gatheral and Jacquier bound.

3.5.3 Calibrating with generalised bounds

Having shown that the generalised bound could lead to superior calibrations at the cost of a higher computational time of the numerical approximation of the bound, we can now look at whether this is true for our `SPX` data set. It can be shown that for our chosen function for $\varphi(\theta)$, the butterfly conditions are essentially a bound on η, where the Gatheral and Jacquier bound is:

$$\begin{cases} \eta < \frac{2\theta_{max}^{\lambda-1/2}}{\sqrt{1+|\rho|}} & \text{if } \theta \leq \frac{4}{1+|\rho|} \\ \eta \leq \frac{4\theta_{max}^{\lambda-1}}{1+|\rho|} & \text{if } \theta \geq \frac{4}{1+|\rho|}, \end{cases} \tag{3.44}$$

with θ_{max} again the value of θ_t corresponding to the last maturity given in the market. The generalised bound gives:

$$\eta \leq \theta_{max}^{\lambda-1/2} \sqrt{\inf_{z\in Z_+(\theta_{max})} \Lambda(\theta_{max}, z)}, \tag{3.45}$$

which we need to derive numerically. For the `SPX` data, the calibrated values $\eta = 0.929$, $\theta_{max} = 0.134$, $\lambda = 0.449$ and $\rho = -0.852$ were found. This means that the Gatheral and Jacquier bound for η equals 1.62, which is still quite a bit above the optimal η. The generalised bound can be found to equal 2.58 here. Clearly as required, the generalised bound is less strict, but either choice would have resulted in the same optimal solution.

We will show that this is generally the case in practice, meaning that we will opt for the computationally easier Gatheral and Jacquier bounds for the remainder of the thesis. However, we advise practitioners using SSVI to at the very least check their results with the generalised bounds in order to be sure of their results.

3.6 Evolution of SSVI parameters

A final aspect of SSVI worth investigating is how the model parameters change over time, especially in times of high and low volatility. For this purpose we used daily `AEX` data over a six month time period and calibrated the SSVI parameters for each of the available days. We plotted the evolution of the individual parameters over time and look for possible patterns that emerge. The particular period we have chosen is from June 15th to December 15th of 2015. The reason for this is that a crisis broke out in China in August of that year, meaning that we would expect the market to display higher volatility around that time. In Figure 3.6 the `AEX` spot price is displayed. It shows that the price indeed experienced a dip due to the China crisis between August and October. Now, we check whether SSVI shows similar instability here.

First, we look at θ_t. Since these parameters correspond to the ATM volatility at a given maturity, we choose the first common maturity of all daily data sets, which in this case was

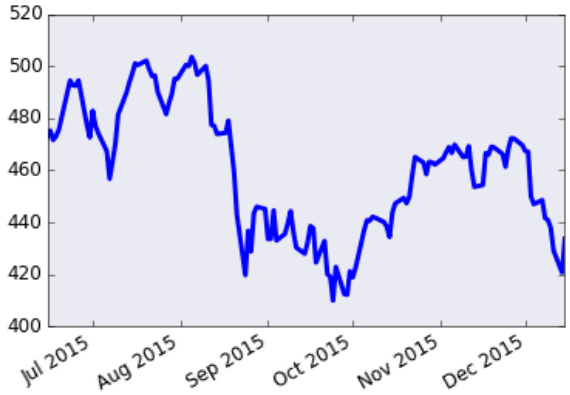

Figure 3.6: AEX spot price from June to December 2015.

December 18th 2015. In Figure 3.7 the evolution of this θ_t parameter is given. Instinctively, one would expect the graph to be a steadily decreasing line as the volatility becomes smaller as the maturity date draws near. This is practically the case here as well, except during the crisis period, where θ_t shows a spike. This follows our intuition, as market uncertainty directly translates to higher ATM volatilities.

Figure 3.7: Plot of θ_t for maturity at December 18th 2015.

The parameters η, λ and ρ are calibrated on each daily data set resulting in a daily parameter set, which are plotted over time. We included the daily error, or the average distance per maturity of the model prices with respect to the market prices in bps of the forward price. Figure 3.9 displays the evolution of all these parameters. This figure shows the effect the crisis has on the model, as during the crisis period the model error is substantially higher than otherwise. From the plots of η, λ and ρ however, we do not observe a pattern emerging. Figure 3.8 shows that the change in these parameters is practically constant, and that the crisis has no real effect here.

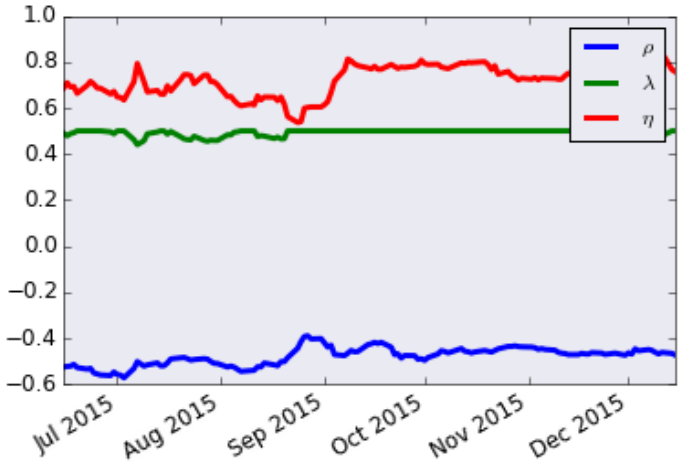

Figure 3.8: η, λ and ρ evolution over time.

3.7 Summary

In this chapter we have taken a closer look at SSVI and the aspects surrounding it. We started with a successful calibration of the model on `SPX` data. Subsequently, we derived new discrete conditions for calendar spread for the model which in the continuous case equated to the conditions set by Gatheral and Jacquier. We showed that, using generalized SSVI, the original butterfly arbitrage conditions were too strict and could be loosened to theoretically improve the model. However, we found that in practice the original bounds were fine as a bound for our chosen function $\varphi(\theta)$, as in most cases this bound was never even close to being infringed. Lastly we showed how the model parameters behave over time especially during a crisis period. We saw that in general the model showed little change over time, except that the model error and the value of θ_t, where normally relatively steady, saw a significant rise during crisis periods.

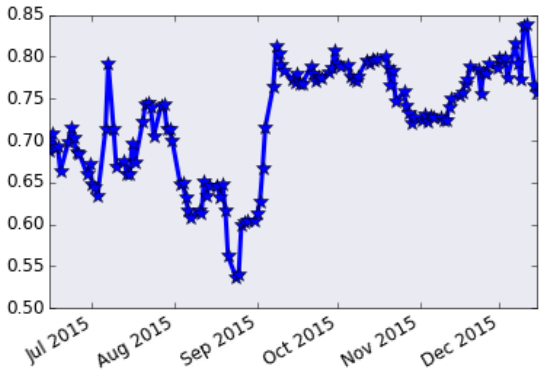

(a) η evolution

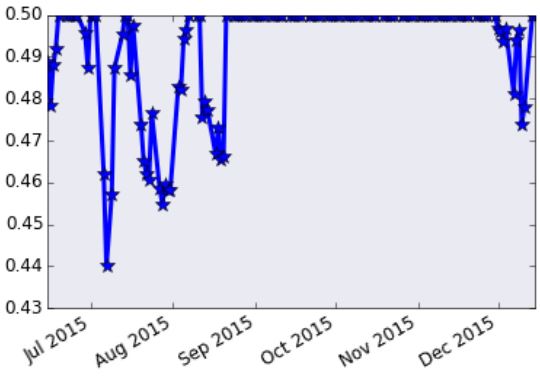

(b) λ evolution

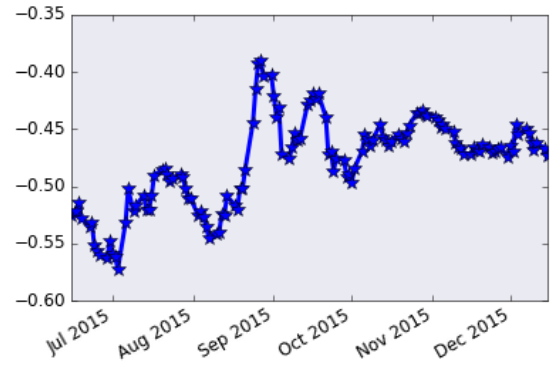

(c) ρ evolution

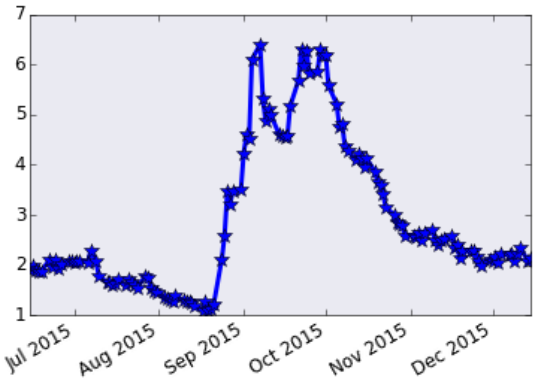

(d) Model error evolution

Figure 3.9: The evolution of SSVI parameters over time.

Chapter 4

The eSSVI surface

Having explored possibilities to improve SSVI itself through arbitrage conditions, we now enhance the model by enlarging the level of freedom in its parameters. One of the limiting factors of the SSVI surface is that the correlation, ρ, is assumed constant over time. Generally, we can be quite certain this is not the case, allowing us to introduce an extension of SSVI, called eSSVI, or extended Surface SVI. The model is nearly identical to SSVI, except that the constant value ρ is replaced by a function: $\rho : \mathbb{R}_+^* \to (-1, 1)$, such that:

$$w(k, \theta_t) = \frac{\theta_t}{2}\left(1 + \rho(\theta_t)\varphi(\theta_t)k + \sqrt{(\varphi(\theta_t)k + \rho(\theta_t))^2 + (1 - \rho(\theta_t))^2}\right). \tag{4.1}$$

Our goal is to find necessary and sufficient conditions for this model to be free of static arbitrage.

Concerning butterfly arbitrage, nothing has changed in this new model. Since butterfly arbitrage is linked to the derivative of the model with respect to the log moneyness k, changing ρ to a function that depends on θ_t does not change anything.

It is more complicated for the calendar-spread arbitrage conditions. A similar method used to find conditions as in Theorem 2.5.1 does not work for this case. To determine these conditions, we again need discrete conditions for all pairs of slices and use these to find the conditions for a continuous function $\rho(\theta_t)$. Subsequently, the model can be calibrated on the same data set as used for SSVI to compare the quality of both models. We finish the chapter by examining the evolution of the eSSVI parameters over time.

4.1 Discrete eSSVI calendar spread arbitrate conditions

Here, by following a similar structure as in Section 3.2, we will derive discrete conditions to prevent calendar spread arbitrage in the new eSSVI model. As before, we will need conditions to ensure that any two eSSVI slices do not intersect. This means that for two eSSVI smiles $w_1 = w(k, \theta_{t_1})$ and $w_2 = w(k, \theta_{t_2})$, using a simplified notation with $\theta_i := \theta_{t_i}$, $\varphi_i := \varphi_(\theta_i)$ and also $\rho_i := \rho(\theta_i)$:

$$\begin{aligned} w_1 &= \frac{\theta_1}{2}(1 + \rho_1\varphi_1 k + \sqrt{\varphi_1^2 k^2 + 2\rho_1\varphi_1 k + 1}), \\ w_2 &= \frac{\theta_2}{2}(1 + \rho_2\varphi_2 k + \sqrt{\varphi_2^2 k^2 + 2\rho_2\varphi_2 k + 1}). \end{aligned}$$

We need $w_2 \geq w_1$ for all k:

$$\theta_2(1+\rho_2\varphi_2 k+\sqrt{\varphi_2^2k^2+2\rho_2\varphi_2 k+1}) \geq \theta_1(1+\rho_1\varphi_1 k+\sqrt{\varphi_1^2k^2+2\rho_1\varphi_1 k+1}). \tag{4.2}$$

For the points $k=0$ and $k=\pm\infty$, this means:

$$\begin{cases} \theta_2 \geq \theta_1 & \text{when } k=0, \\ \theta_2\varphi_2(1+\rho_2) \geq \theta_1\varphi_1(1+\rho_1) & \text{when } k=\infty, \\ \theta_2\varphi_2(1-\rho_2) \geq \theta_1\varphi_1(1-\rho_1) & \text{when } k=-\infty. \end{cases} \tag{4.3}$$

Again, since it is assumed that all $\rho_i \in (-1,1)$, we get: $\frac{\theta_2}{\theta_1} \geq 1$, $\frac{\theta_2\varphi_2}{\theta_1\varphi_1} \geq \frac{1+\rho_1}{1+\rho_2}$ and $\frac{\theta_2\varphi_2}{\theta_1\varphi_1} \geq \frac{1-\rho_1}{1-\rho_2}$.

Writing: $x := \varphi_1 k$, $\theta := \frac{\theta_2}{\theta_1}$, $\varphi := \frac{\varphi_2}{\varphi_1}$, we get:

$$\theta(1+\rho_2\varphi x+\sqrt{\varphi^2x^2+2\rho_2\varphi x+1}) \geq (1+\rho_1 x+\sqrt{x^2+2\rho_1 x+1}), \tag{4.4}$$

and our conditions read:

$$\theta \geq 1,\ \theta\varphi \geq \frac{1+\rho_1}{1+\rho_2} \text{ and } \theta\varphi \geq \frac{1-\rho_1}{1-\rho_2}. \tag{4.5}$$

So the question is: assuming the previous conditions hold, is the inequality (4.4) in force, or do we need additional conditions?

4.1.1 Roots of a fourth degree polynomial:

Again, the inequality (4.4) is rewritten as $\alpha+\theta z_2 \geq z_1$ where:

$$\begin{aligned} \alpha &:= \theta(1+\rho_2\varphi x)-(1+\rho_1 x) = \theta-1+(\theta\rho_2\varphi-\rho_1)x, \\ z_1 &:= \sqrt{x^2+2\rho_1 x+1} \text{ and } z_2 := \sqrt{\varphi^2x^2+2\rho_2\varphi x+1}. \end{aligned}$$

To analyse if the opposite can be true, we look at the root of the equality:

$$\alpha+\theta z_2 = z_1. \tag{4.6}$$

By squaring twice, we get the function P:

$$P := 4\alpha^2\theta^2 z_2^2-(z_1^2-\alpha^2-\theta^2 z_2^2)^2 = 0, \tag{4.7}$$

where any root of (4.6) is also a root of P, and if at least two of these roots exist, the slices intersect and calendar spread arbitrage exists. For any root of P, we again have the same three possibilities:

$$\begin{cases} 2\alpha\theta z_2 = -(z_1^2-\alpha^2-\theta^2 z_2^2) & \text{or,} \\ 2\alpha\theta z_2 = z_1^2-\alpha^2-\theta^2 z_2^2 \text{ and } \alpha+\theta z_2 = -z_1 & \text{or,} \\ 2\alpha\theta z_2 = z_1^2-\alpha^2-\theta^2 z_2^2 \text{ and } \alpha+\theta z_2 = z_1, & \end{cases} \tag{4.8}$$

where only the last case corresponds to an intersection of slices.

Filling in the values for α, z_1 and z_2, the polynomial P becomes:

$$\begin{aligned} P(x) &= -\left((\rho_1-\theta\varphi\rho_2)^2-(\theta\varphi-1)^2\right)\left((\rho_1-\theta\varphi\rho_2)^2-(\theta\varphi+1)^2\right)x^4 \\ &\quad +4\theta\left((\rho_1+\varphi\rho_2)((\rho_1-\theta\varphi\rho_2)^2-\theta^2\varphi^2-1)+2\theta\varphi(\varphi\rho_1+\rho_2)\right)x^3 \\ &\quad +4\theta(\theta-1)(\rho_1^2-\theta\varphi^2\rho_2^2+\theta\varphi^2-1)x^2. \end{aligned}$$

Here x^2 is a factor of P, which can again be dropped as $x=0$ is not a root of (4.6). Hence, a second order polynomial Q remains, where:

$$P = x^2 Q. \tag{4.9}$$

4.1.2 Study of the roots of Q

By setting this function $Q(x)$ equal to zero, the discriminant is obtained:

$$D = 16\theta(\rho_1^2\theta^2\varphi^2\rho_2^2+\theta^2\varphi^2 1)^2((\rho_1\theta\varphi\rho_2)^2-(\theta-1)(\theta\varphi^2-1)). \tag{4.10}$$

The discriminant of Q is positive, and so two real roots exist, if and only if:

$$(\rho_1-\theta\varphi\rho_2)^2-(\theta-1)(\theta\varphi^2-1)>0. \tag{4.11}$$

If we define: $Z(x)=z_1^2-\theta z_2^2-\alpha^2$, we can see that non zero roots x_1,x_2 of $Q(x)$ also correspond to roots of (4.6) if $Z(x)\alpha<0$, or when $\alpha\geq 0$ and $\theta z_2+\alpha>0$.

Roots as a function of ρ_1 and ρ_2

Clearly, Q only has two real roots on the domain we call I of all $\boldsymbol{\rho}=(\rho_1,\rho_2)$ with $\rho_1,\rho_2\in(-1,1)$ such that (4.11) holds. We define $\boldsymbol{\rho}^*=\left\{\boldsymbol{\rho}:((\rho_1-\theta\varphi\rho_2)^2-(\theta-1)(\theta\varphi^2-1)=0\right\}$. If we let x be a root of Q, with $\boldsymbol{\rho}$ in this domain, this can be written as:

$$\begin{aligned} x_{\boldsymbol{\rho}} &= \frac{2\theta\left((\rho_1+\varphi\rho_2)((\rho_1-\theta\varphi\rho_2)^2-\theta^2\varphi^2-1)+2\theta\varphi(\varphi\rho_1+\rho_2)\right)}{((\rho_1-\theta\varphi\rho_2)^2-(\theta\varphi-1)^2)((\rho_1-\theta\varphi\rho_2)^2-(\theta\varphi+1)^2)} \\ &\quad \pm\frac{2(\rho_1^2-\theta^2\varphi^2\rho_2^2-\theta^2\varphi^2+1)\sqrt{\theta\left((\rho_1-\theta\varphi\rho_2)^2-(\theta-1)(\theta\varphi^2-1)\right)}}{\left((\rho_1-\theta\varphi\rho_2)^2-(\theta\varphi-1)^2\right)\left((\rho_1-\theta\varphi\rho_2)^2-(\theta\varphi+1)^2\right)}. \end{aligned}$$

Using this value of $x_{\boldsymbol{\rho}}$, explicit expressions for α and Z can be obtained, namely $\alpha(x_{\boldsymbol{\rho}})$ and $Z(x_{\boldsymbol{\rho}})$. Furthermore, we also see that, since under (4.5) $(\rho_1-\theta\varphi\rho_2)^2<(\theta\varphi-1)^2,(\theta\varphi+1)^2$, they are all continuous functions of $\boldsymbol{\rho}$.

Lemma 4.1.1. *$(\rho_1,\rho_2)\to\alpha(x_{\boldsymbol{\rho}})Z(x_{\boldsymbol{\rho}})$ does not change sign for $\rho_1,\rho_2\in(-1,1)$.*

Proof. Assume the opposite, meaning that a change of sign requires that $\alpha(x_{\boldsymbol{\rho}})Z(x_{\boldsymbol{\rho}})=0$ for some $\boldsymbol{\rho}$. Since: $2\alpha\theta z_2=\pm Z$, we see that $Z(x_{\boldsymbol{\rho}})=0\Leftrightarrow\alpha(x_{\boldsymbol{\rho}})=0$, so if $\alpha(x_{\boldsymbol{\rho}})=Z(x_{\boldsymbol{\rho}})=0$:

$$\begin{aligned} &\begin{cases} z_1^2-\theta^2z_2^2=0 \\ \theta(1+\rho_2\varphi x)=1+\rho_1 x \end{cases} \quad\Rightarrow\quad \begin{cases} \theta^2(\varphi^2x^2+2\rho_2\varphi x+1)=x^2+2\rho_1x+1 \\ \theta^2(\rho_2^2\varphi^2x^2+2\rho_2\varphi x+1)=\rho_1^2x^2+2\rho_1x+1 \end{cases} \\ &\Rightarrow\quad (1-\rho_2^2)\theta^2\varphi^2x^2=(1-\rho_1^2)x^2 \qquad \text{(subtracting the two equations)} \\ &\Leftrightarrow\quad \theta^2\varphi^2=\frac{1-\rho_1^2}{1-\rho_2^2}. \end{aligned}$$

Under condition (4.5) this means that: $\theta\varphi=\frac{1+\rho_1}{1+\rho_2}=\frac{1-\rho_1}{1-\rho_2}$. Hence: $\rho_1=\rho_2=1$, which contradicts their definition. □

Lemma 4.1.2. *For $\boldsymbol{\rho}^*$ as defined above, $Z(x_{\boldsymbol{\rho}^*})$ is strictly negative, and since $\alpha(x_{\boldsymbol{\rho}^*}) \geq 0 \Leftrightarrow 0 < \varphi \leq 1$, it holds that: $\alpha(x_{\boldsymbol{\rho}^*})Z(x_{\boldsymbol{\rho}^*}) < 0 \Leftrightarrow 0 < \varphi \leq 1$.*

Proof. First off, note that when $\varphi = 1$, it is certain that the slices do not cross, as we never have two roots, since this requires: $(\rho_1 - \theta\rho_2)^2 > (\theta - 1)^2$, which is never true. From now on, we look at every $\varphi \neq 1$. We also see that when $\varphi < 1$ it is possible that $\theta\varphi^2 - 1 < 0$, meaning that we always have that $(\rho_1 - \theta\varphi\rho_2)^2 - (\theta - 1)(\theta\varphi^2 - 1) > 0$, thus we always have two roots for any values of $\rho_1, \rho_2 \in (-1, 1)$ and $\boldsymbol{\rho}^*$ does not exist. If we thus in this case set $\boldsymbol{\rho}^* = (0, 0)$, we see that $\alpha(x_{\boldsymbol{\rho}^*}) = \theta - 1$, $z_1 = \sqrt{x_{\boldsymbol{\rho}^*}^2 + 1}$ and $z_2 = \sqrt{\varphi^2 x_{\boldsymbol{\rho}^*}^2 + 1}$. Hence: $\alpha(x_{\boldsymbol{\rho}^*}) > 0$ always holds and:

$$Z(x_{\boldsymbol{\rho}^*}) = x_{\boldsymbol{\rho}^*}^2(\theta\varphi^2 - 1) - \theta(\theta - 1) < 0, \tag{4.12}$$

also always holds. If however for $\varphi < 1$ it holds that $\theta\varphi^2 - 1 > 0$, then $\boldsymbol{\rho}^*$ always exists, and if we now define $y^2 := (\rho_1 - \theta\varphi^2) = (\theta - 1)(\theta\varphi^2 - 1)$ we can find:

$$\begin{aligned} x_{\boldsymbol{\rho}^*} &= \frac{2\theta\left((\rho_1 + \varphi\rho_2)((\rho_1 - \theta\varphi\rho_2)^2 - \theta^2\varphi^2 - 1) + 2\theta\varphi(\varphi\rho_1 + \rho_2)\right)}{((\rho_1 - \theta\varphi\rho_2)^2 - (\theta\varphi - 1)^2)((\rho_1 - \theta\varphi\rho_2)^2 - (\theta\varphi + 1)^2)} \\ &= \frac{2(\theta\varphi\rho_2 - \varphi\rho_2 + y)}{(\varphi - 1)(\varphi + 1)}. \end{aligned}$$

For our function $Z(x) = z_1^2 - \alpha^2 - \theta^2 z_2^2$, we can see that:

$$\begin{aligned} Z(x) &= x^2 + 2\rho_1 x + 1 - (\theta - 1 - (\rho_1 - \theta\varphi\rho_2)x)^2 - \theta^2(\varphi^2 x^2 + 2\varphi\rho_2 x + 1) \\ &= x^2\left(-(\rho_1 - \theta\varphi\rho_2)^2 - \theta^2\varphi^2 + 1\right) + 2\theta x\left((\rho_1 - \theta\varphi\rho_2) - \rho_2\varphi(\theta - 1)\right) - 2\theta(\theta - 1). \end{aligned}$$

Now, if we fill $x_{\boldsymbol{\rho}^*}$ into this equation, we get:

$$Z(x_{\boldsymbol{\rho}^*}) = -\frac{2\theta(\theta - 1)}{(\varphi - 1)^2(\varphi + 1)^2}\left((2\varphi y + \rho_2(2\theta\varphi^2 - \varphi^2 - 1))^2 + (1 - \rho_2^2)(\varphi - 1)^2(\varphi + 1)^2\right), \tag{4.13}$$

which is always negative, regardless of the sign of y or ρ_2.

Now, we will look at $\alpha(x_{\boldsymbol{\rho}^*})$, which can be written as: $\theta - 1 - xy$. If we fill in our value for $x_{\boldsymbol{\rho}^*}$, we get:

$$\alpha(x_{\boldsymbol{\rho}^*}) = -\frac{\theta - 1}{(\varphi - 1)(\varphi + 1)}(2\varphi\rho_2 y + 2\theta\varphi^2 - \varphi^2 - 1). \tag{4.14}$$

From this, it follows that, if $\theta > 1$ and $0 < \varphi < 1$: $\alpha(x_{\boldsymbol{\rho}^*}) > 0 \Leftrightarrow \frac{2\varphi\rho_2 y + 2\theta\varphi^2 - \varphi^2 - 1}{\varphi - 1} < 0$. However, it can be shown that the numerator is always strictly positive, since this is equivalent to:

$$(\theta\varphi^2 - 1) + \varphi^2(\theta - 1) > -2\varphi\rho_2 y, \tag{4.15}$$

where we know the LHS of this inequality is always positive. So either the RHS is negative, and it is true, or it is positive. In the latter case, squaring results in:

$$4\theta^2\varphi^4 - 4\theta\varphi^4 - 4\theta\varphi^2 + \varphi^4 + 2\varphi^2 + 1 > 4\varphi^2\rho_2^2(\theta^2\varphi^2 - \theta\varphi^2 - \theta + 1)$$
$$\Leftrightarrow 4\varphi^2(\theta-1)(\theta\varphi^2-1)(1-\rho_2^2) + (\varphi^2-1)^2 > 0$$

Since this last inequality always holds, we can conclude that $\alpha(x_{\boldsymbol{\rho}^*}) > 0 \Leftrightarrow \varphi < 1$. Combining this with the result for $Z(x_{\boldsymbol{\rho}^*})$ provides the required result. □

By combining Lemmas 4.1.1 and 4.1.2, we see that if we have that our necessary conditions from (4.5) and $\varphi \leq 1$ hold that always $\alpha(x)Z(x) < 0$. This would mean that in this case the slices never intersect. Next we look at what happens when $\varphi > 1$.

Lemma 4.1.3. *If P has any root $x_{\boldsymbol{\rho}}$, then: $(\alpha + \theta z_2)(x_{\boldsymbol{\rho}}) > 0 \Leftrightarrow \varphi > 1$.*

Proof. We start by showing that the function $x_{\boldsymbol{\rho}} \to (\alpha + \theta z_2)(x_{\boldsymbol{\rho}})$ never changes sign. This is clear, since if the opposite were true, by its continuity there would exist ρ_1, ρ_2 such that $(\alpha + \theta z_2)(x_{\rho_1,\rho_2}) = 0$. However, (4.6) then implies that: $z_1(x_{\rho_1,\rho_2}) = 0$, which is impossible since $\rho_1, \rho_2 \in (-1, 1)$.

Knowing this, we look at the value of $(\alpha + \theta z_2)(x_{\boldsymbol{\rho}^*})$ to see whether this function is always positive or negative. We find that:

$$\begin{aligned}(\alpha + \theta z_2)(x_{\boldsymbol{\rho}^*}) &= \theta\left(\frac{\sqrt{(2\varphi y + \rho_2(2\theta\varphi^2 - \varphi^2 - 1))^2 + (\varphi^2-1)^2(1-\rho_2^2)} - 2\varphi\rho_2 y - 2\theta\varphi^2 + \varphi^2 + 1}{\varphi^2 - 1}\right) \\ &\quad + \frac{2\varphi\rho_2 y + 2\theta\varphi^2 - \varphi^2 - 1}{\varphi^2 - 1},\end{aligned}$$

First off, from the proof of Lemma 4.1.2 it follows that $\frac{2\varphi\rho_2 y + 2\theta\varphi^2 - \varphi^2 - 1}{\varphi^2 - 1} > 0 \Leftrightarrow \varphi > 1$. We can also find that: $\sqrt{(2\varphi y + \rho_2(2\theta\varphi^2 - \varphi^2 - 1))^2 + (\varphi^2-1)^2(1-\rho_2^2)} - 2\varphi\rho_2 y - 2\theta\varphi^2 + \varphi^2 + 1 = 0$, since:

$$\begin{aligned}\sqrt{(2\varphi y + \rho_2(2\theta\varphi^2 - \varphi^2 - 1))^2 + (\varphi^2-1)^2(1-\rho_2^2)} &= 2\varphi\rho_2 y + 2\theta\varphi^2 - \varphi^2 - 1 \\ \Leftrightarrow\ (2\varphi y + \rho_2(2\theta\varphi^2 - \varphi^2 - 1))^2 + (\varphi^2-1)^2(1-\rho_2^2) &= (2\varphi\rho_2 y + 2\theta\varphi^2 - \varphi^2 - 1)^2 \\ \Leftrightarrow\ 4\varphi^2(y^2 - \theta^2\varphi^2 + \theta\varphi^2 + \theta - 1)(1-\rho_2^2) &= 0,\end{aligned}$$

where the second step of squaring both sides is allowed since it is known from previous results that both sides are always positive. Since $y^2 = \theta^2\varphi^2 - \theta\varphi^2 - \theta + 1$, we see that this final equality holds. Combining this gives: $(\alpha + \theta z_2)(x_{\boldsymbol{\rho}^*}) > 0 \Leftrightarrow \varphi > 1$ and the result then follows. □

From all this, we can now summarize the cases for our eSSVI model when roots of Q are also roots of (4.6) and therefore cause the slices to cross with the following proposition:

Proposition 4.1.4. *Assume $\theta > 1$ and $\theta\varphi > \max\left(\frac{1+\rho_1}{1+\rho_2}, \frac{1-\rho_1}{1-\rho_2}\right)$. Then the smiles intersect if and only if:*

$$\varphi > 1 \text{ and } (\rho_1 - \theta\varphi\rho_2)^2 > (\theta-1)(\theta\varphi^2 - 1). \tag{4.16}$$

4.1.3 eSSVI discrete calendar spread conditions

First of all, the necessary conditions: $\theta \geq 1$ and $\theta\varphi > \max\left(\frac{1+\rho_1}{1+\rho_2}, \frac{1-\rho_1}{1-\rho_2}\right)$, must always hold to allow $w_2 \geq w_1$. Next, to ensure that the smiles do not cross, it is required that:

- $\varphi \leq 1$, or,
- $(\rho_1 - \theta\varphi\rho_2)^2 \leq (\theta - 1)(\theta\varphi^2 - 1)$.

4.2 Graphical illustration

Just as with SSVI, we will here give a quick illustration of these conditions. Naturally, we will ensure that (4.5) always holds. We give four figures of pairs of eSSVI slices in Figure 4.1.

Figure 4.1 (a) displays eSSVI slices where we have that: $\theta = \varphi = 2$, $\rho_1 = -1/2$ and $\rho_2 = 6/10$. This means that we have $\theta > 1$, $\theta\varphi > \max\left(\frac{1+\rho_1}{1+\rho_2}, \frac{1-\rho_1}{1-\rho_2}\right)$ and $\varphi > 1$. Proposition 4.1.4 now dictates that the slices cross, which can be seen to be true in the figure, as:

$$(\theta - 1)(\theta\varphi^2 - 1) = 7 \text{ and } (\rho_1 - 3\rho_2)^2 = 8.41$$

so indeed $(\rho_1 - \theta\varphi\rho_2)^2 > (\theta - 1)(\theta\varphi^2 - 1)$.

In Figure 4.1 (b) we now have slices where: $\theta = \varphi = 2$, $\rho_1 = -0.6$ and $\rho_2 = \frac{-\sqrt{7}-0.6}{4}$. This means that: $\varphi > 1$ and $(\rho_1 - \theta\varphi\rho_2)^2 = (\theta - 1)(\theta\varphi^2 - 1)$. Here, the slices in the figure can be seen to only touch but not intersect, in correspondence with Proposition 4.1.4.

For Figure 4.1 (c) we now take: $\theta = \varphi = 2$, $\rho_1 = -0.6$, and $\rho_2 = -\frac{\sqrt{7}}{4}$. This means that: $(\rho_1 - \theta\varphi\rho_2)^2 < (\theta - 1)(\theta\varphi^2 - 1)$. In Figure 4.1 (d) we have: $\varphi = 0.5$, and then $\theta = 5$, $\rho_1 = -\rho_2 = -0.1$, so $\varphi < 1$. According to Proposition 4.1.4, we should have two pairs of slices that never cross, which is true in the figures.

Again, it can be graphically seen from Figure 4.1 that plots follow our proposition on the discrete slices. The smiles only intersect in the case where we expect them to, otherwise they do not.

4.3 Finding continuous conditions

Here, we will examine what happens when the differences between θ_1 and θ_2 become infinitesimally small. This means that: $d\theta = \theta_2 - \theta_1 \Rightarrow \theta_2 = \theta_1 + d\theta$ and $d\theta \to 0$. Again we can now say that for all higher order order terms of $d\theta : \mathcal{O}(d\theta^2) \approx 0$. So in this case, if we call $\theta = \theta_1$, we have: $\frac{\theta_2}{\theta_1} = 1 + \frac{d\theta}{\theta}$. Likewise, we find that, since the function φ is dependent on θ_t, we get that: $\varphi\prime(\theta)d\theta = \varphi_2 - \varphi_1 \Rightarrow \varphi_2 = \varphi_1 + \varphi\prime(\theta)d\theta$, so if again $\varphi = \varphi_1$, we have: $\frac{\varphi_2}{\varphi_1} = 1 + \frac{\varphi\prime(\theta)d\theta}{\varphi}$.

We again define:

$$\gamma := \frac{1}{\varphi}\frac{d(\theta\varphi)}{d\theta} = 1 + \theta\frac{\varphi\prime(\theta)}{\varphi}. \tag{4.17}$$

If we now fill these values into our previously found conditions we can find conditions on these new parameters.

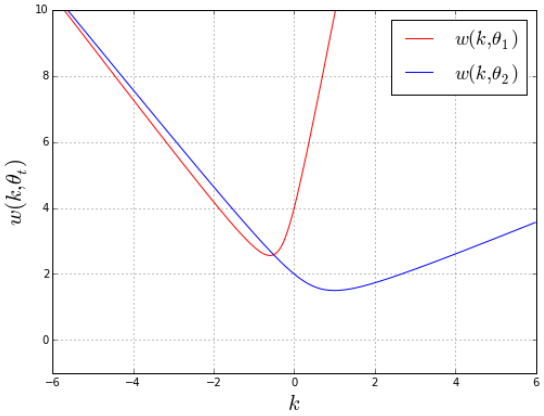

(a) Case where the eSSVI smiles intersect.

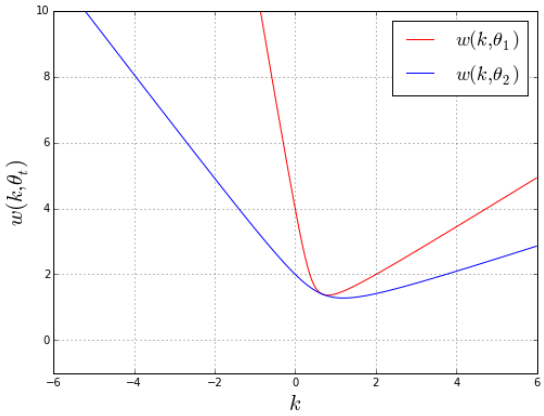

(b) Case where the eSSVI smiles touch, but do not intersect.

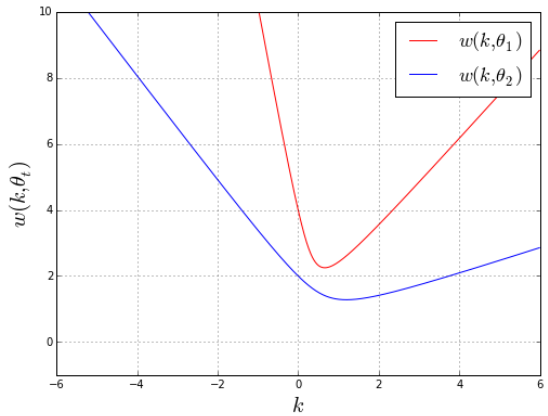

(c) Case where the eSSVI smiles never intersect.

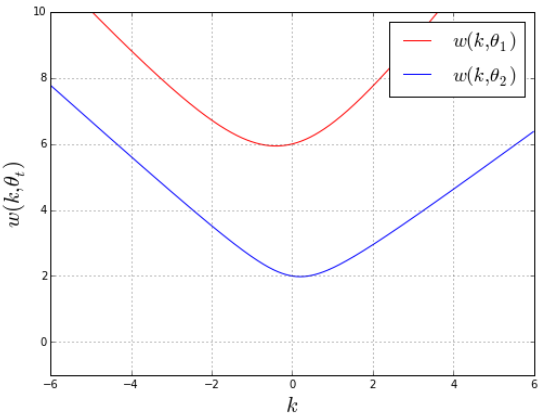

(d) Case where the eSSVI smiles never intersect.

Figure 4.1: Various pairs of eSSVI slices.

4.3.1 Necessary conditions

From (4.5), we see that for the first necessary condition, we require: $\frac{\theta_2}{\theta_1} \geq 1$. This is equivalent to:

$$\frac{\theta_2}{\theta_1} = 1 + \frac{d\theta}{\theta} \geq 1 \Leftrightarrow \frac{d\theta}{\theta} \geq 0 \Leftrightarrow \frac{d\theta}{dt} \geq 0. \tag{4.18}$$

Next, for the second necessary condition:

$$\begin{cases} \theta\varphi \geq \frac{1-\rho_1}{1-\rho_2}, \\ \theta\varphi \geq \frac{1+\rho_1}{1+\rho_2} \end{cases} . \tag{4.19}$$

We set: $\rho_1 = \rho$, and $\rho_2 = \rho + \rho\prime(\theta)d\theta$. Apart from this, it is known that: $\theta\varphi = \left(1 + \frac{d\theta}{\theta}\right)\left(1 + \frac{\varphi\prime(\theta)}{\varphi}d\theta\right) = 1 + \gamma\frac{d\theta}{\theta}$. Plugging this into equations (4.18) and (4.19), we get:

$$\begin{cases} 1 + \gamma\frac{d\theta}{\theta} \geq \frac{1-\rho}{1-\rho-\rho\prime(\theta)d\theta}, \\ 1 + \gamma\frac{d\theta}{\theta} \geq \frac{1+\rho}{1+\rho+\rho\prime(\theta)d\theta}, \end{cases} \tag{4.20}$$

or:

$$\begin{cases} 1-\rho-\rho\prime(\theta)d\theta+(1-\rho)\gamma\frac{d\theta}{\theta}+\mathcal{O}(d\theta^2)\geq 1-\rho, \\ 1+\rho+\rho\prime(\theta)d\theta+(1+\rho)\gamma\frac{d\theta}{\theta}+\mathcal{O}(d\theta^2)\geq 1+\rho. \end{cases} \tag{4.21}$$

This is equivalent to

$$\begin{cases} (-\theta\rho\prime(\theta)+(1-\rho)\gamma)\frac{d\theta}{\theta}\geq 0, \\ (\theta\rho\prime(\theta)+(1+\rho)\gamma)\frac{d\theta}{\theta}\geq 0. \end{cases} \tag{4.22}$$

Now, given that $d\theta/\theta > 0$, and defining:

$$\delta := \theta\rho\prime(\theta). \tag{4.23}$$

we can write:

$$\begin{cases} \delta\leq(1-\rho)\gamma, \\ \delta\geq-(1+\rho)\gamma. \end{cases} \tag{4.24}$$

So, in this case, the new necessary conditions are: $\frac{d\theta}{dt}\geq 0$ and $-\gamma\leq\delta+\rho\gamma\leq\gamma$.

4.3.2 Secondary conditions

Besides these necessary conditions, we saw from Proposition 4.1.4 that the smiles did not cross if either: $\varphi\leq 1$ or $(\rho_1-\theta\varphi\rho_2)^2\leq(\theta-1)(\theta\varphi^2-1)$. So in this infinitesimal case we get:

$$\begin{aligned} 1+\frac{\varphi\prime(\theta)}{\varphi}d\theta\leq 1 &\Leftrightarrow \frac{\varphi\prime(\theta)}{\varphi}\leq 0 \\ &\Leftrightarrow 1+\theta\frac{\varphi\prime(\theta)}{\varphi}\leq 1 \\ &\Leftrightarrow \gamma\leq 1. \end{aligned}$$

Next, if we write: $\rho_1=\rho$ and $\rho_2=\rho+\rho\prime(\theta)d\theta$, we get:

$$\begin{aligned} (\rho-(\rho+\rho\prime(\theta)d\theta)\theta\varphi)^2 &\leq (\theta-1)(\theta\varphi^2-1) \\ \Leftrightarrow(\rho(1-\theta\varphi)-\theta\varphi\rho\prime(\theta))^2 &\leq (\theta-1)(\theta\varphi^2-1). \end{aligned}$$

Like in the previous cases, when we substitute θ and φ with $(1+\frac{d\theta}{\theta})$ and $(1+\frac{\varphi\prime(\theta)}{\varphi}d\theta)$ respectively, we get that: $(1-\theta\varphi)=-\frac{d\theta}{\theta}\gamma$, $(\theta-1)=\frac{d\theta}{\theta}$ and $(\theta\varphi^2-1)=\frac{d\theta}{\theta}(2\gamma-1)$.

Filling this into the equation above results in:

$$\begin{aligned} \left(-\rho\gamma\frac{d\theta}{\theta}-\left(\gamma\frac{d\theta}{\theta}+1\right)\rho\prime(\theta)d\theta\right)^2 &\leq \left(\frac{d\theta}{\theta}\right)^2(2\gamma-1) \\ \Leftrightarrow\left(\frac{d\theta}{\theta}\right)^2(-\rho\gamma-\theta\rho\prime(\theta))^2+\mathcal{O}((d\theta)^4) &\leq \left(\frac{d\theta}{\theta}\right)^2(2\gamma-1). \end{aligned}$$

By eliminating the higher order term of $d\theta$ as these are negligible, and by cancelling out $(d\theta/\theta)^2$ and using $\delta:\theta\rho\prime(\theta)$, this can be rewritten as:

$$\delta^2 + 2\rho\gamma\delta + (\rho^2\gamma^2 - 2\gamma + 1) \leq 0, \tag{4.25}$$

where this inequality is only true when δ lies between the roots of this polynomial, so:

$$\delta_{1,2} = \frac{-2\rho\gamma \pm \sqrt{4\rho^2\gamma^2 - 4\rho^2\gamma^2 + 8\gamma - 4}}{2} = -\rho\gamma \pm \sqrt{2\gamma - 1}. \tag{4.26}$$

Here, the condition becomes: $-\sqrt{2\gamma - 1} \leq \delta + \rho\gamma \leq \sqrt{2\gamma - 1}$.

4.3.3 eSSVI continuous calendar spread conditions

Our necessary conditions resulted in: $\frac{d\theta}{dt} > 0$ and $-\gamma \leq \delta + \rho\gamma \leq \gamma$, where we defined: $\gamma := \frac{\partial_\theta(\theta\varphi(\theta)}{\varphi(\theta)}$ and $\delta := \theta\partial_\theta\rho(\theta)$. This implies that we require $\gamma \geq 0$. Besides this, we also require that either:

- $\gamma \leq 1$ or,
- $-\sqrt{2\gamma - 1} \leq \delta + \rho\gamma \leq \sqrt{2\gamma - 1}$.

These conditions can be used to find calendar spread arbitrage conditions for any choice of functions $\varphi(\theta)$ and $\rho(\theta)$.

4.4 Parametric eSSVI calibration

As with SSVI, we now go through the steps required to calibrate the eSSVI model to real market data. We again derive parameters that minimize the total distance between the market prices, and those implied by our model as described in (3.1). In terms of data, the same data set of `SPX` option prices on 22/02/16 is used. However, to do this we must first make a choice of functions for $\varphi(\theta)$ and $\rho(\theta)$ and use our newly found conditions to find restrictions on their parameters in order to ensure the absence of static arbitrage. As before, we will use the power-law form for φ, so: $\varphi(\theta) = \eta\theta^{-\lambda}$. After some testing, we have found that at least for `SPX` data, the function $\rho(\theta) = a\exp(-b\theta) + c$ performs well.

For our calendar spread arbitrage conditions, we now look at the conditions derived in Section 4.3.3. It is known that $\gamma = 1 - \lambda$, therefore if we take $\lambda \in [0, 1]$ we only need to prove that:

$$|\delta + \rho\gamma| \leq \gamma. \tag{4.27}$$

For the chosen functions of $\varphi(\theta)$ and $\rho(\theta)$, this can be written as:

$$\left|\left(a - \frac{ab\theta}{1-\lambda}\right)\exp(-b\theta) + c\right| \leq 1. \tag{4.28}$$

The LHS only has a single extremum at $\theta = \frac{2-\lambda}{b}$. Hence, we only need to check whether the statement holds at the extremum, and for $\theta = 0$ and $\theta \to \infty$, leading to:

$$\begin{cases} |c - \frac{a}{1-\lambda}\exp(\lambda - 2)| \leq 1, \\ |a + c| \leq 1, \\ |c| \leq 1. \end{cases} \tag{4.29}$$

These last two conditions conveniently correspond to the conditions that $\rho(0)$ and $\lim_{\theta\ to\infty}\rho(\theta)$ both lie in $[-1,1]$. In an optimal solution, we need to ensure that these condition hold for these parameters.

For butterfly arbitrage, we have that:

$$\eta \leq \max_{0\leq\theta_t\leq\theta_N}\left(\frac{4\theta_t^{\lambda-1}}{1+|\rho(\theta_t)|}, \frac{2\theta_t^{\lambda-1/2}}{\sqrt{1+|\rho(\theta_t)|}}\right), \tag{4.30}$$

where again N is the time of the last maturity. If we make sure that all these conditions hold in an optimal solution, it follows that the implied volatility surface will be completely free of static arbitrage.

Clearly, for the same data set, the values of θ_t are the same for eSSVI as they were for SSVI. However, by changing ρ from a constant value to a function of θ_t, it can safely be assumed that the parameters for λ and η also change. After calibrating and ensuring arbitrage-freeness through the conditions above, the functions for φ and ρ are obtained and plotted in Figure 4.2. The exact functions are:

$$\varphi(\theta_t) = 0.84\theta_t^{-0.48} \text{ and } \rho(\theta_t) = 0.33e^{-248.7\theta_t} - 0.86. \tag{4.31}$$

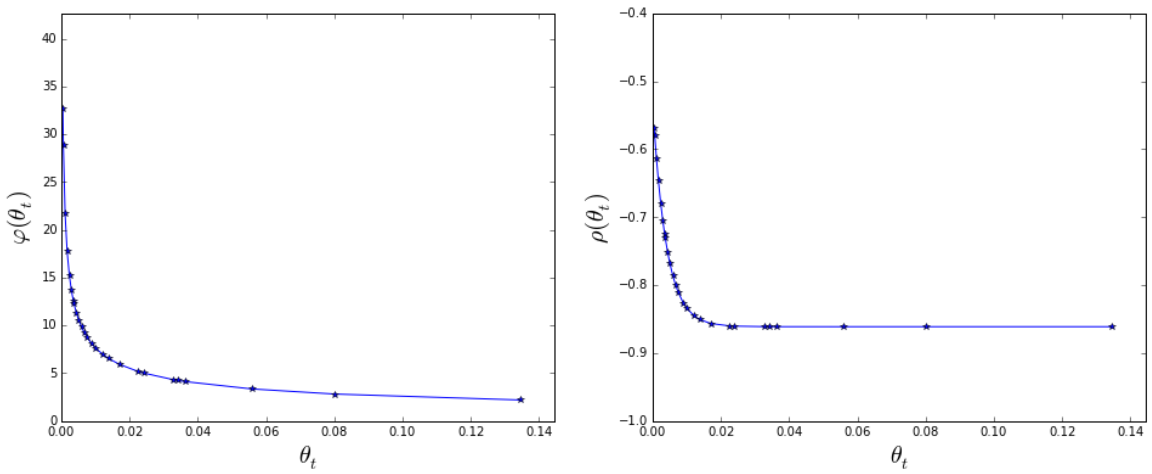

Figure 4.2: Plot of the calibrated functions $\varphi(\theta_t)$ and $\rho(\theta_t)$.

In Figure 4.3, where we show the implied volatility smile given by eSSVI for the first, middle and last maturity are compared to the market bid and ask volatility. At first glance it appears that little has changed for the new model.

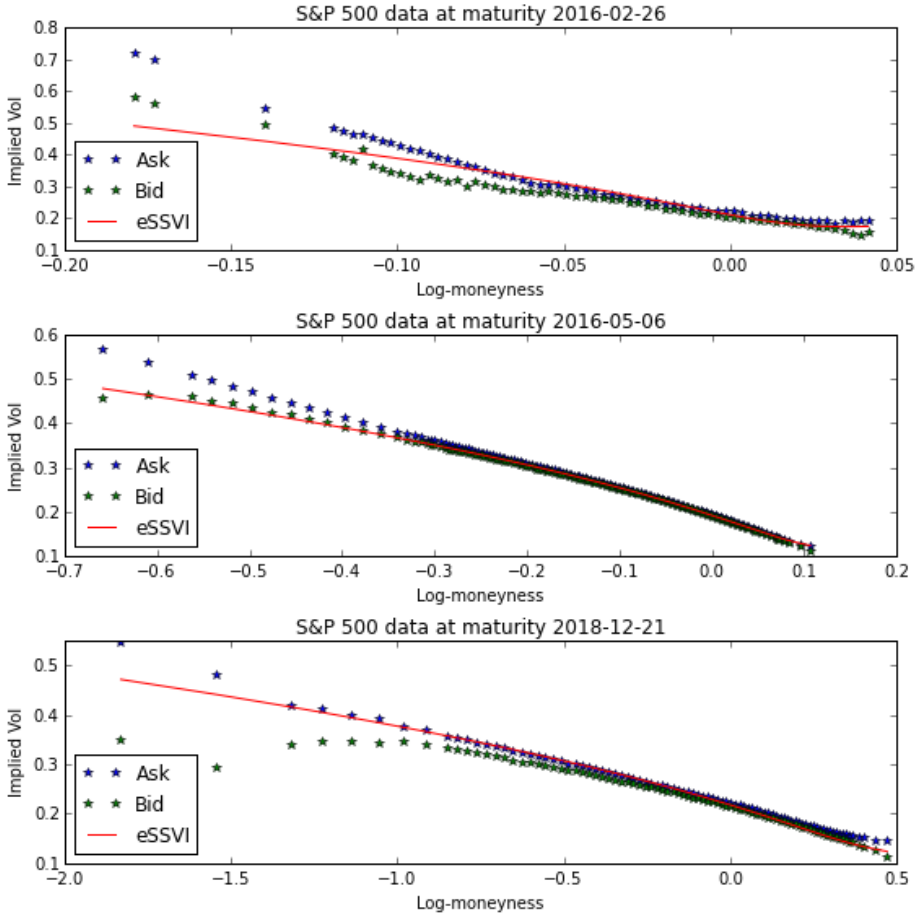

Figure 4.3: Market bid and ask and eSSVI volatility smiles for the first, middle and last maturity.

In Table 4.2 the 2-norm distances of the model and market price in bps of the forward price are given. We see that the fit follows the market well, only the last two maturities going over 0.5. As our main concern was to improve on the SSVI model, we compare the results of both models in order to get a better idea of the impact of the change to a non-constant ρ.

i	1	2	3	4	5	6	7	8	9	10	11	12	13
D_i	0.245	0.253	0.199	0.186	0.122	0.139	0.111	0.126	0.117	0.010	0.088	0.071	0.076
i	14	15	16	17	18	19	20	21	22	23	24	25	26
D_i	0.094	0.181	0.111	0.227	0.262	0.312	0.375	0.371	0.387	0.359	0.101	0.563	2.528

Table 4.1: Table of distances of calibrated eSSVI model to the data per maturity

4.5 Parametric SSVI vs eSSVI

By combining the results of the two calibrations, the two models can be compared. First, the difference in the functions of φ and ρ is shown in Figure 4.4. First, we have the two

functions for φ, which we found were $0.93\theta_t^{-0.45}$ for SSVI and $0.84\theta_t^{-0.48}$ for eSSVI. The plot shows that there is hardly any difference here. For ρ, we found the constant value in SSVI of: $\rho = -0.85$ and the function found for eSSVI: $\rho(\theta_t) = 0.33e^{-248.7\theta_t} - 0.86$. From Figure 4.4 we see that this constant value is somewhat of an weighted average of our function over the given values of θ_t. Here, it is clear that one would expect an increase in accuracy for eSSVI for the early maturities as the distance here between the SSVI and eSSVI ρ is greatest.

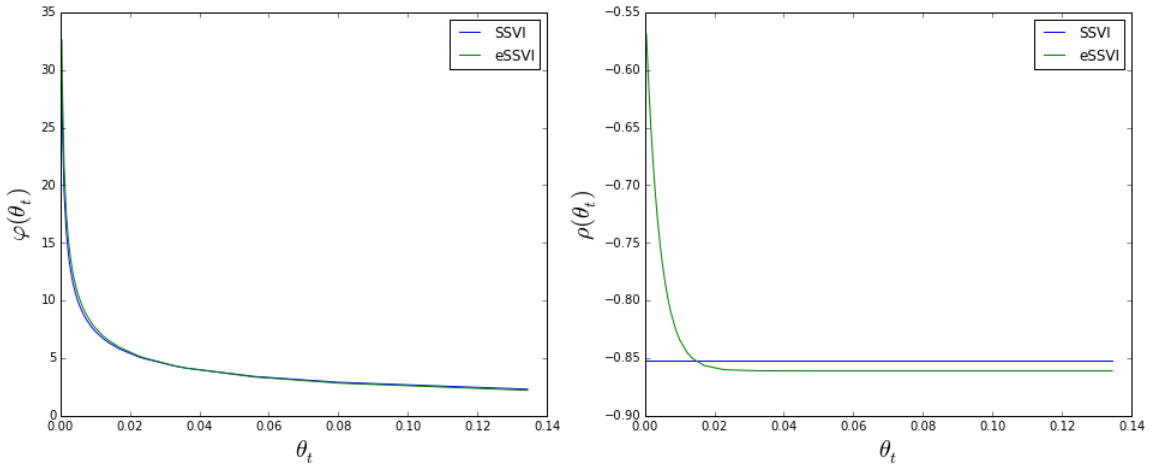

Figure 4.4: Comparison of the calibrated functions of $\varphi(\theta_t)$ and $\rho(\theta_t)$ for SSVI and eSSVI.

Next, we plot the model implied volatilities and the market bid and ask volatilities for the first, middle and last maturity in Figure 4.5. Here, we see a better performance for eSSVI on the first maturity for positive log-moneynesses. However, apart from this, graphically, we cannot directly conclude a better performance for the new model.

Lastly, the 2-norm differences in model and market price are combined in Table 4.2 and also the factor for how much smaller the eSSVI distance is than the SSVI distance. We see that for the first couple of maturities, this factor is approximately 2, indicating that there is a substantial improvement. Over the whole set of maturities,an approximate improvement of factor 1.5 is observed. Since there is little additional computational cost required for eSSVI with respect to SSVI, we conclude that, so far, the new eSSVI model would be a better choice in modelling the implied volatility surface.

i	1	2	3	4	5	6	7	8	9	10	11	12	13
D_i	0.463	0.456	0.392	0.385	0.268	0.268	0.212	0.223	0.168	0.125	0.090	0.070	0.071
D_i	0.245	0.253	0.199	0.186	0.122	0.139	0.111	0.126	0.117	0.010	0.088	0.071	0.076
Factor	1.89	1.80	1.97	2.07	2.20	1.94	1.91	1.77	1.43	1.26	1.03	0.98	0.93
i	14	15	16	17	18	19	20	21	22	23	24	25	26
D_i	0.113	0.258	0.172	0.404	0.467	0.497	0.594	0.492	0.533	0.463	0.126	0.758	3.076
D_i	0.094	0.181	0.111	0.227	0.262	0.312	0.375	0.371	0.387	0.359	0.101	0.563	2.528
Factor	1.21	1.42	1.54	1.78	1.78	1.59	1.58	1.33	1.38	1.29	1.25	1.35	1.22

Table 4.2: Table of distances of both the SSVI and eSSVI model to the data per maturity.

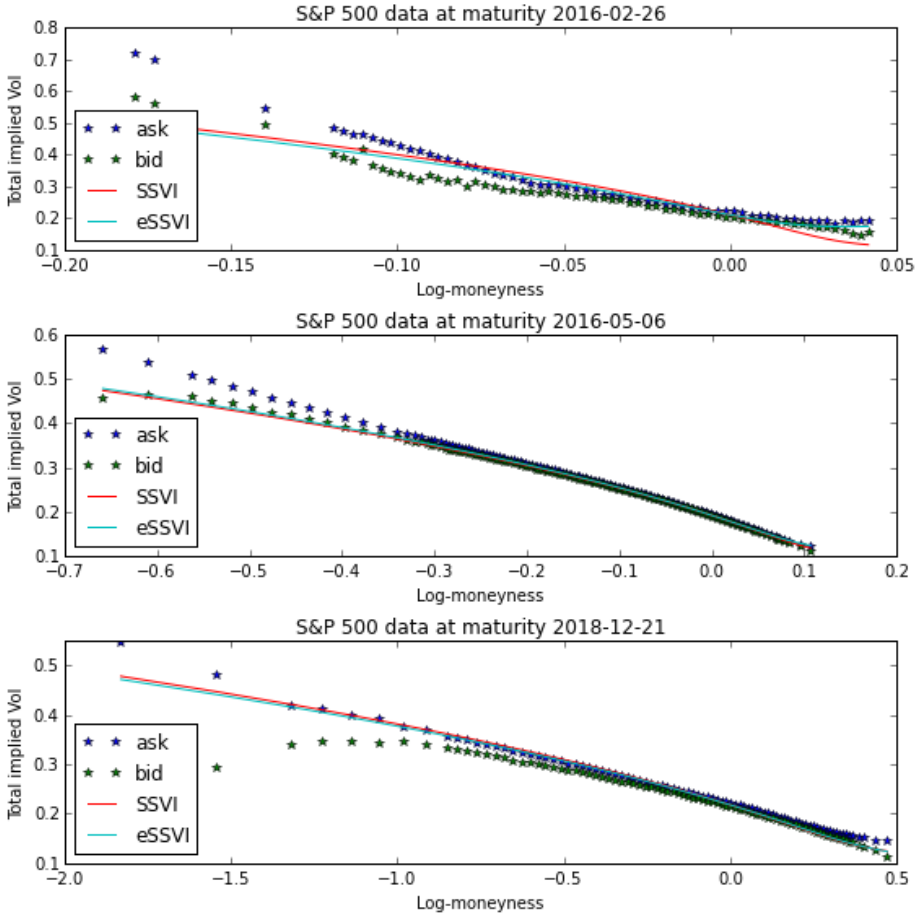

Figure 4.5: Market bid and ask and SSVI and eSSVI volatility smiles for the first, middle and last maturity.

4.6 Evolution of eSSVI parameters

Just as with SSVI we can evaluate the eSSVI parameters over the same period of `AEX` data from June 15th to December 15th 2015. Since the models both have the same values for θ_t, these values will follow the same path as plotted in Figure 3.7, and still have the same spike of θ_t values during the crisis period.
From Figure 4.7 no real pattern can be observed from the paths of the parameters over time. All appear somewhat random and do not show any change during the crisis time or otherwise. The only noteworthy aspect comes from the graph for the model error. Where with SSVI we saw a clear spike in model error during the crisis period, eSSVI has no such feature. There is only one small spike in October, where we believe that the model had an error in its calibration or the daily data displayed some kind of irregularity. This fact that the model still performs well during times of high volatility can be very valuable and is another advantage for eSSVI.

In Figure 4.6,the four parameters η, λ, a and c are plotted together. We see that the parameters for ρ display some irregularity during the same time we had our spike in model error. Another possible reason for this is that the chosen parametrization for $\rho(\theta)$ does not

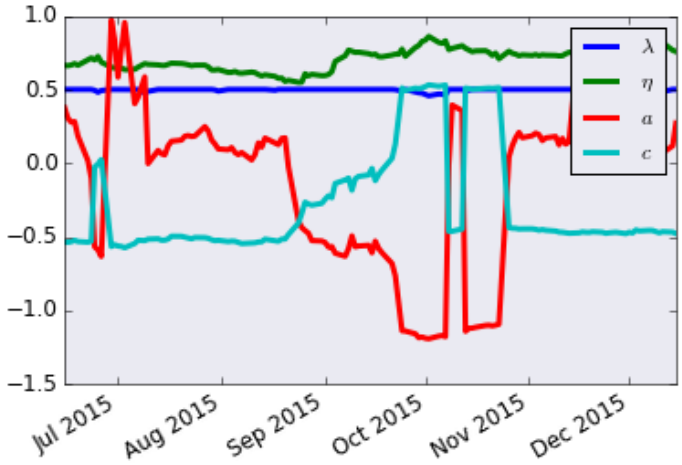

Figure 4.6: η, λ, a and c evolution over time.

work as well here and perhaps a better choice is possible.

4.7 Summary

We introduced an extension to SSVI, eSSVI with a non-constant ρ, with both the new discrete and continuous parameters for the model. Using this, we calibrated the model on the same `SPX` data as before and compared the two models. We observed that especially for early maturities eSSVI performed better than SSVI. Finally, we discussed the evolution of the model parameters.

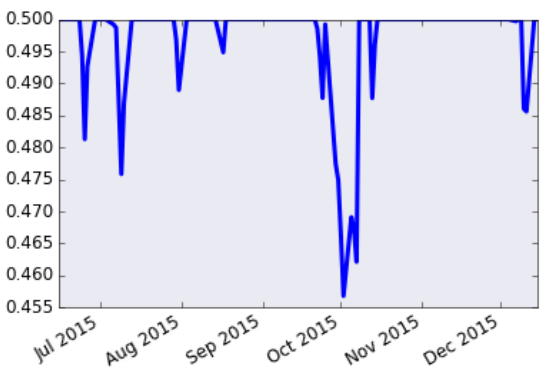

(a) η evolution

(b) λ evolution

(c) a evolution

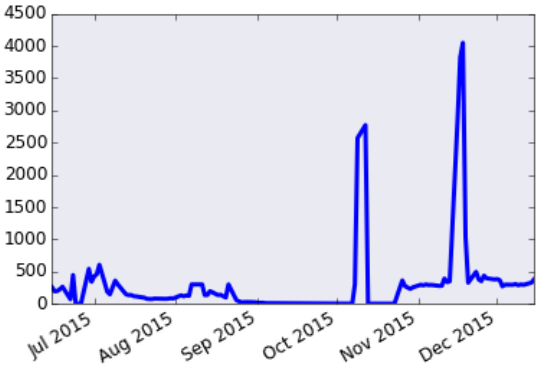

(d) b evolution

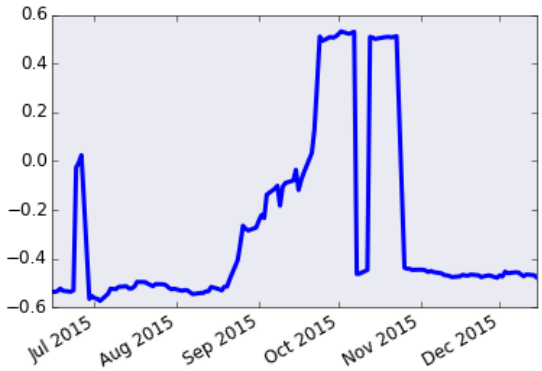

(e) c evolution

(f) Model error evolution

Figure 4.7: The evolution of eSSVI parameters over time

Chapter 5

Local volatility and American options

In the previous chapters we have only considered the most basic European options. Due to the very simple form of the Black-Scholes formula, the clear link between implied volatilities and option prices allows for an easy transformation between the two. This is no longer the case when we consider more complex exotic options. Generally there is no analytic formulation of exotic option prices, so numerical approximation of these prices is needed to calibrate the volatility surface. This is the main goal in this chapter.

First, local volatilities are considered, a tool that is most often used in the pricing of exotic and American options. The advantage of using local volatilities is that there is a known formulation of this local volatility in terms of a volatility surface such as SSVI. After this derivation, we look at the method that this local volatility is generally used in to price path-dependent options like American options, namely the trinomial tree. Using all of this, we can calibrate both the SSVI and eSSVI surface on American option data and compare the two results.

5.1 Local volatility

As mentioned, implied volatility models aim to find value that, when inserted in Black-Scholes formula, gives a correct price for a given European option. Under the Black-Scholes assumptions, which we now know are not observable in the real market, it was assumed that the stock price S_t had the following dynamics:

$$dS_t = rS_t dt + \sigma dW_t, \tag{5.1}$$

where W_t is a Brownian motion under the risk-free measure and σ the volatility assumed constant over time. Note that this is not the case in the market. Instead, it was found that one can get correct prices if they substitute this constant volatility with a function of the time and spot price called the local volatility: $\sigma_{loc}(S,t)$. Dupire [6] was among the first to find a relation between this local volatility and an option price $C(T,K)$. Here he found that from the PDE for this option price, one can derive:

$$\frac{\partial C}{\partial T} = \frac{1}{2}\sigma_{loc}^2 K^2 \frac{\partial^2 C}{\partial K^2}. \tag{5.2}$$

Inverting this gives an expression for the value of the local volatility which has been dubbed the *Dupire formula*:

$$\sigma_{loc}^2(T,K) = \frac{2\frac{\partial C}{\partial t}(T,K)}{\frac{\partial^2 C}{\partial K^2}(T,K)}. \tag{5.3}$$

An issue with this formulation is that it requires the use of finite differences on a limited number of strikes and option prices given in the market. For this reason, the formula has been transformed to a function of the volatility surface, like SSVI for example.

5.2 SSVI equivalent local volatility

5.2.1 Dupire formula in total variance

Since the pricing of exotic options is often done through the use of local volatility, it is now our goal to find a way to calibrate local volatilities on market data using Dupire's formula in (5.3). Luckily, this can be transformed to a formula with implied total variance surfaces such as SSVI. As shown by Gatheral [10], for a volatility surface w defined as:

$$w(k,t) = \sigma_{BS}^2(k,t)t, \tag{5.4}$$

with t the time to maturity and $k = \log(K/F_t)$ the logmoneyness, results in:

$$\sigma_{loc}^2(k,t) = \frac{\frac{\partial w}{\partial t}}{\left(1 - \frac{kw'(k)}{2w(k)}\right)^2 - \frac{w'(k)^2}{4}\left(\frac{1}{w(k)} + \frac{1}{4}\right) + \frac{w''(k)}{2}} = \frac{\frac{\partial w}{\partial t}}{g(k)}, \tag{5.5}$$

where $\sigma_{loc}(k,t)$ is the local volatility we are looking for.
It should be noted that the static arbitrage conditions for w are in essence present in the definition of local volatility, as essentially it requires both:

$$\frac{\partial w}{\partial t} \geq 0 \text{ and } g(k) \geq 0. \tag{5.6}$$

5.2.2 Application to SSVI

Using SSVI as the parametrization of the volatility surface, so with:

$$w(\theta_t,k) = \frac{\theta_t}{2}\left(1 + \rho\varphi(\theta_t)k + z\right), \tag{5.7}$$

where for ease of notation $z := \sqrt{\varphi(\theta_t)^2k^2 + 2\rho\varphi(\theta_t)k + 1}$, we can compute explicitely:

$$\begin{aligned}
\frac{\partial w}{\partial t} &= \frac{1}{2}\left(1 + \frac{1+\rho\varphi(\theta_t)k}{z} + k\partial_\theta(\theta_t\varphi(\theta_t))\left(\frac{\varphi(\theta_t)k+\rho}{z} + \rho\right)\right)\frac{\partial\theta}{\partial t},\\
g(k) &= a(x) - b(x)\theta\varphi(\theta_t)^2 - \frac{c(x)}{16}\theta^2\varphi(\theta_t)^2,
\end{aligned}$$

where a, b and c are functions that depend only on $x := \varphi(\theta_t)k$. It can be shown that:

$$\begin{aligned}
w'(k) &= \frac{\theta_t\varphi(\theta_t)}{2}\left(\rho + \frac{\varphi(\theta_t)k+\rho}{z}\right),\\
w''(k) &= \frac{\theta_t\varphi(\theta_t)^2}{2}\frac{1-\rho^2}{z^3}.
\end{aligned}$$

Using this, analytic expressions for a, b and c can be derived:

$$\begin{aligned}
a(x) &= \left(1 - \frac{kw'(k)}{2w(k)}\right)^2 = \left(1 - \frac{k\left(\rho + \frac{k\varphi(\theta_t)+\rho}{z}\right)}{2(1+\rho\varphi(\theta_t)k+z)}\right)^2 = \frac{1}{4}\left(1+\frac{1}{z}\right)^2, \\
b(x)\theta_t\varphi(\theta_t)^2 &= \frac{w'(k)^2}{4w(k)} - \frac{w''(k)}{2} \\
\Leftrightarrow b(x) &= \ldots = \frac{z^2 + (2\rho^2 + \rho x - 1)z - 2(1-\rho^2)}{2z^3}, \\
c(x)\theta^2\varphi(\theta_t)^2 &= w'(k)^2 \Leftrightarrow c(x) = \frac{1}{4}\left(\rho + \frac{\varphi(\theta_t)k+\rho}{z}\right)^2 = \frac{(x+\rho+\rho z)^2}{4z^2}.
\end{aligned}$$

Which result in:

$$\sigma^2_{loc} = \frac{\left(1 + \frac{1+\rho\varphi(\theta_t)k}{z} + k\partial_\theta(\theta_t\varphi(\theta_t))\left(\frac{\varphi(\theta_t)k+\rho}{z} + \rho\right)\right)\frac{\partial\theta}{\partial t}}{2a(x) - 2b(x)\theta_t\varphi(\theta_t) - \frac{c(x)}{8}\theta_t^2\varphi(\theta_t)^2}. \tag{5.8}$$

5.2.3 The SSVI local volatility at extreme values

By enforcing the static arbitrage conditions, one can be sure that both $\partial w/\partial t$ and $g(k)$ are always non-negative, which ensure that σ^2_{loc} is never assigned a negative value. In addition to this, since we saw from the generalized butterfly arbitrage conditions that the conditions conditions given by Gatheral and Jacquier in Theorem 2.5.2 are only sufficient as here we always have that $g(k) > 0$, we also know that under these conditions there are never singularities in (5.5).

Here, we will examine two cases. First, when θ goes to zero. This is of interest as then much of the formula is simplified, which is especially true since we will later find that only the case where also $k = 0$ is needed for our computations. Next, we examine the behaviour of the local volatility in the wings, i.e. when $k \to \pm\infty$.

If we take $k = 0$ in (5.8) and then evaluate the limit of $\theta_t \to 0$, so also $t \to 0$, we get:

$$\lim_{t\to 0}\sigma^2_{loc}(k,t) = \lim_{\theta_t\to 0}\frac{\frac{\partial w}{\partial\theta_t}(\theta_t,0)\frac{d\theta_t}{dt}}{g(0)}, \tag{5.9}$$

where:

$$\frac{\partial w}{\partial\theta_t}(\theta_t,0) = 1 \text{ and } g(0) = \frac{4\theta_t\varphi(\theta_t)^2 - 8\theta_t\varphi(\theta_t)^2\rho^2 - \theta_t^2\varphi(\theta_t)^2\rho^2 + 16}{16}. \tag{5.10}$$

Due to the butterfly arbitrage condition, we know that $\lim_{\theta\to 0}\theta\varphi(\theta)^2 = 0$ and that $\lim_{\theta\to 0}\theta^2\varphi(\theta)^2 = c$, where $c \geq 0$. This means that:

$$\lim_{\theta_t\to 0} g(0) = \frac{16 - (8+\rho^2)c}{16}. \tag{5.11}$$

However, it is well known property of the local volatility that here we should have that:

$$\lim_{t\to 0}\sigma^2_{loc}(t,0) \approx \lim_{t\to 0}\sigma^2_{BS}(t,0). \tag{5.12}$$

However, from the definition of θ_t, we see that:

$$\lim_{t\to 0}\frac{d\theta_t}{t}=\lim_{t\to 0}\frac{d(t\sigma^2_{BS}(t,0)}{dt}=\lim_{t\to 0}\sigma^2_{BS}(t,0), \tag{5.13}$$

we see that:

$$\lim_{t\to 0}\sigma^2_{loc}(t,0)=\lim_{t\to 0}\frac{d\theta_t}{t} \tag{5.14}$$

Therefore, we require: $\lim_{\theta\to 0}\theta^2\varphi(\theta)^2=0$.

This fact causes a small problem with SSVI. If one takes $\varphi(\theta)=\eta\theta^{-\lambda}$, where $\eta>0$ and $\lambda\in[0,1/2]$, the surface is arbitrage free, however:

$$\lim_{\theta\to 0}\theta^2\varphi(\theta)^2=\lim_{\theta\to 0}\eta^2\theta^{2\lambda-1}=\begin{cases}0 & \text{if } \lambda<1/2\\ \eta^2 & \text{if } \lambda=1/2\end{cases}. \tag{5.15}$$

This limit goes to zero as required when $\lambda<1/2$, however, when $\lambda=1/2$ we have that: $\lim_{t\to 0}\sigma^2_{loc}(t,0)>\lim_{\theta_t\to 0}d\theta_t/dt$. Mathematically, this should not be possible for arbitrage-free surfaces. Unfortunately, we have not found a proper reason for this phenomenon. We will therefore list this as possible future research and proceed by limiting $\lambda\in[0,1/2)$ in order to avoid this.

To examine the behaviour of the local volatility in the wings we look at what happens when $k\to\pm\infty$, so we find:

$$\begin{aligned}\lim_{k\to\pm\infty}w(k) &= \frac{\theta\varphi}{2}k(\rho\pm 1),\\ \lim_{k\to\pm\infty}w'(k) &= \frac{\theta\varphi}{2}(\rho\pm 1) \text{ and } \lim_{k\to\pm\infty}w''(k)=0,\end{aligned}$$

therefore:

$$\lim_{k\to\pm\infty}g(k)=\frac{1}{4}-\frac{\theta^2\varphi^2(1\pm\rho)^2}{64}. \tag{5.16}$$

This means that, by simplifying with: $\gamma=\partial_\theta(\theta\varphi(\theta))/\varphi(\theta)$, we get for the local volatility:

$$\lim_{k\to\pm\infty}\sigma^2_{loc}=\frac{64\lim_{k\to\pm\infty}\frac{\partial w}{\partial t}}{16-\theta^2\varphi^2(\rho\pm 1)^2}=\frac{32\lim_{k\to\pm\infty}(1\pm\rho+k\varphi\gamma(\rho\pm 1))\frac{\partial\theta}{\partial t}}{16-\theta^2\varphi^2(1\pm\rho)^2}\to\pm\infty. \tag{5.17}$$

However, we can clearly see that the local volatility goes to infinity in the wings at the rate $\sqrt{k}$, as $\lim_{k\to\pm\infty}\frac{\sigma^2_{loc}}{k}=\frac{\varphi\gamma(\rho\pm 1)\partial_t\theta}{16-\theta^2\varphi^2(1\pm\rho)^2}$, is a constant in k.

5.2.4 Difference implied and local volatility

With all this, we can now examine an example where an SSVI volatility surface is transformed to a local volatility surface. We will use the parameters found from the `SPX` data used earlier, so where $\rho=-0.85$ and $\varphi(\theta)=0.93\theta^{-0.45}$. In Figure 5.1 we have both the

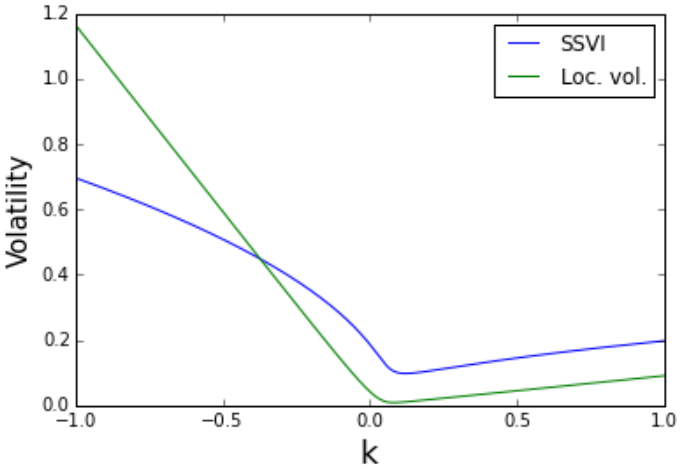

Figure 5.1: Difference between an SSVI slice and the corresponding local volatiltiy.

Black-Scholes implied volatility σ_{BS}, where $w_{SSVI}(\theta_t, k) = t\sigma^2_{BS}(t,k)$, and the SSVI equivalent local volatility σ_{loc} for $\theta_t = 0.0024$. Clearly, the dynamics of the local volatility are much different than that of implied volatility.
Now we consider the trinomial tree, which is the method we will be using with our newly found local volatility to price exotic options.

5.3 Local vol trinomial tree

One of the first pricing methods taught to finance students is the binomial tree, where the price path over a discrete time period is examined. However, this method is slow and outdated, being mostly replaced with the so-called trinomial tree. As explained by Derman [5] the idea is that, if we start with a spot price S, it can only move to one of three nodes: with probability p to the *up* node $S_u = S \cdot U$, with probability q to the *down* node $S_d = S \cdot D$ and with probability $1 - p - q$ to middle node $S_m = S \cdot M$. Hence, there are five unknown parameters per time step: the two probabilities p and q and the up, down and middle ticks U, D and M. We say that $U > M > D$, as when this order is different we can get it again by renaming the ticks, and if any are equal we are in the case of a binomial tree, which we want to avoid. This process then continues per time step. A graphical representation of a single time step can be found in Figure 5.2.
It should be noted that it is assumed that both the risk-free rate and the dividends are zero in this case, but the method can easily be altered such that these values are taken into account. There are two conditions on these parameters, namely that the first and second moments of the price process must match that of a geometric Brownian motion. Hence, we need:

$$\begin{aligned} pS_u + qS_d + (1-p-q)S_m &= S \\ p(S_u - S)^2 + q(S_d - S)^2 + (1-p-q)(S_m - S)^2 &= S^2\sigma^2_{loc}\Delta t + \mathcal{O}(\Delta t^2). \end{aligned}$$

To simplify matters, we assume the tree is recombining, which means that: $S_m = S$, therefore: $M = 1$ and $U \cdot D = 1$. Hence, if we substitute $S_u = S \cdot U$ and $S_d = S \cdot D$ this

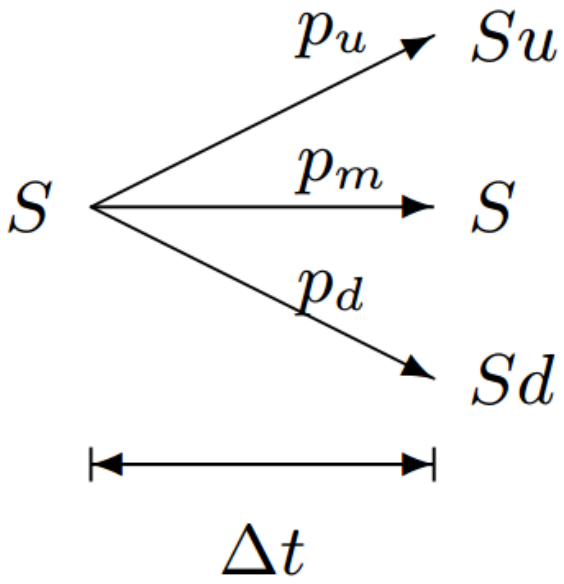

Figure 5.2: A single trinomial tree time step.

gives:

$$\begin{aligned} pU + qD &= p + q \\ p(U-1)^2 + q(D-1)^2 &\approx S^2\sigma_{loc}^2\Delta t. \end{aligned}$$

If U and D are known, the values for p and q are:

$$p = \frac{\sigma_{loc}^2\Delta t}{(U-1)(U-D)} \text{ and } q = \frac{\sigma_{loc}^2\Delta t}{(1-D)(U-D)}. \tag{5.18}$$

These values for p and q are always positive as required, however we still need to ensure that $m = 1 - p - q$ is also positive. This is true when:

$$\sigma_{loc}^2\Delta t \leq (U-1)(1-D). \tag{5.19}$$

This condition should hold at every step of the tree, meaning that:

$$\tau := \sup_{(t,S)\in Tree} \sigma_{loc}^2\Delta t \leq (U-1)(1-D). \tag{5.20}$$

After some basic algebra and using $UD = 1$, the following condition is obtained:

$$U \geq 1 + \frac{\tau}{2} + \sqrt{(1+\frac{\tau}{2})^2 - 1} \tag{5.21}$$

Since the idea of the trinomial tree is that it convergences to a diffusion model when we take a small enough time step, we take U of the form: $\exp \sigma_g\sqrt{\Delta t}$. This σ_g is so-called *generator volatility*, a constant in the tree that is a rough estimate of the local volatility. Filling this new value of U into (5.21) when $\sup_{(t,S)\in \text{Tree}} \sigma_{loc}^2$ is bounded, and when Δt goes to zero, we can find a condition on the local volatility in terms of this generator volatility. In this case, it rewrites to: $U \geq 1 + \sqrt{\tau}$ or yet by using the Taylor expansion for U:

$$\sigma_g^2 \geq \sup_{(t,S)\in Tree} \sigma_{loc}^2. \tag{5.22}$$

If this holds, we are sure that all probabilities are between zero and one, resulting in a correct tree.

5.3.1 Bounded local vol

From the behaviour of the SSVI equivalent local volatility it was observed that it is not bounded when $k \to \pm\infty$. Similarly, the SSVI surface is not bounded here as well. Both surfaces blow up at a rate of $\sqrt{k}$, meaning that the condition in (5.22) never holds.

This can be solved by saying that the unbounded local volatility does not contribute to the price given by the trinomial tree for extreme values of k. Therefore a so-called cut level in $|k|$ can be introduced such that the local volatility remains constant beyond this level. If this level is chosen high enough, the prices should be very close to the theoretical ones.

Here a level β is set such that the local volatility will be cut at $k = \pm\beta\sqrt{\theta}$, where for $k \geq |\beta\sqrt{\theta}|$ the local volatility is kept constant from here on. Figure 5.3 shows how this cut works in practice. The local volatility blows up for extreme values of k, but the cut manages to keep it bounded. We set the value $\beta = 3.0$ for our cut level.

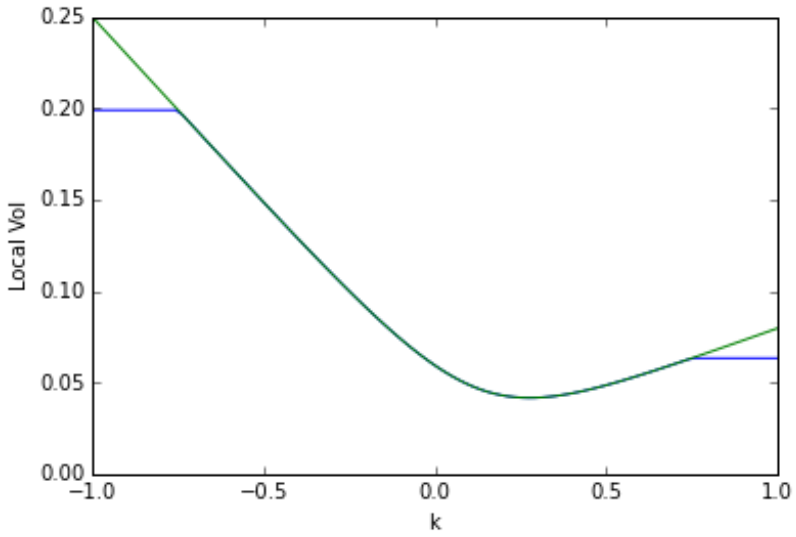

Figure 5.3: Local volatility bounded by a cut

Using this, a trinomial tree can be simulated as a price process S_t taking a set number of time steps N to a maturity T, where when N increases, the closer this simulation will be to a real price path. For the pricing of European options, we can use the following scheme to find the options price for a given strike K. After the final time step, so at $t = T$, we have a list of $S_{T,j}$'s, depending on the route through the tree, where we can find the payoff at these spot prices: $(S_{T,j} - K)^+$. We set this value equal to $C_{N,j}$. We then track back through the tree to $t = 0$ using that:

$$C_{i,j} = pC_{i+1,j+1} + (1 - p - q)C_{i+1,j} + qC_{i+1,j-1}, \tag{5.23}$$

resulting in a value for C_0, which is the option price.

Since the holder of an American option can exercise it at any time prior to maturity, these options are slightly trickier. However, as shown in Chapter 7 of Wilmott [16], there is only a single time that early exercise is optimal and that is when one, at that time, can get the same pay-off as one would get at maturity. This means for our tree that we will keep the value of our pay-offs, $C_{N,j}$, and at each time step i check: $\max(pC_{i+1,j+1}+(1-p-q)C_{i+1,j}+qC_{i+1,j-1}, C_{N,j})$. Using this throughout the tree, we can again find our option value C_0 for a given strike K.

Using this method, one can obtain very accurate American option prices corresponding to a local volatility derived from an SSVI or eSSVI surface. Using market data, we can calibrate the volatility surface on the market prices and examine its performance.

5.4 Calibrating American options

With the trinomial tree pricing scheme, the SSVI model can be calibrated on American options. The way this works is that we calibrate our model parameters such that when we plug the resulting SSVI equivalent local volatility in our trinomial tree pricer, the distance between market and model prices is minimal. For the trinomial tree, we will choose the amount of time steps N equal to 100, as this is generally a high enough value such that the tree gives an accurate value, but does not require too much computational time.

It should be noted that we cannot first calibrate the values of θ_t on market implied volatilities as these do not exist for exotic options. The reason for this is obvious, as the Black-Scholes formula no longer applies here, therefore we no longer have an analytic relation between an option price and the volatility. We therefore need to calibrate the θ_t values together with the other parameters under the condition that the θ_t values are strictly increasing in time. A second note is that we also cannot use the put-call parity to find the forward prices and discount factors needed in the trinomial tree. Luckily, the data provided came with heuristically guessed values for both the forward and discount factor, which proved to work well in our calibration.

To examine the models performance, SSVI is calibrated here on `ING` American option data from two days, namely August 14th and 24th 2016. Since we have seen that SSVI performs worse during a crisis, these dates are chosen as they represent a day before the crisis and the day the crisis started. After optimizing the SSVI parameters to minimize the distance between market and model prices, we derive the values of θ_t given in Figure 5.4. We see that this is again nearly a straight line and very similar to the values found in the European case in Figure 3.1.

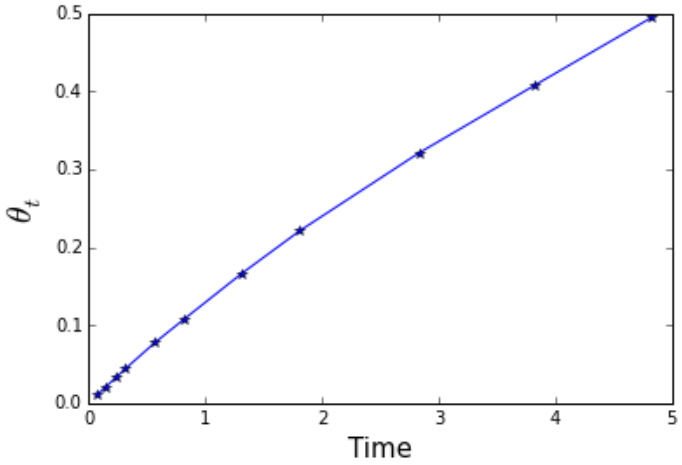

Figure 5.4: Plot of the calibrated θ_t values

For the remaining parameters, we derive that $\eta = 0.871$, $\lambda = 0.496$ and $\rho = -0.545$. This results in the function $\varphi(\theta)$ shown in Figure 5.5.

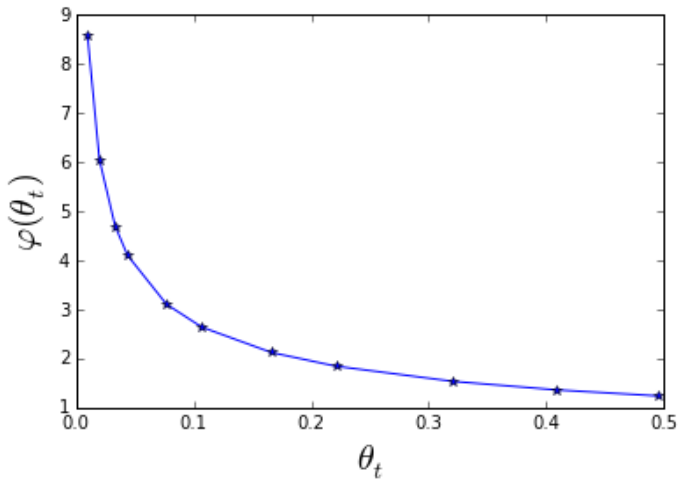

Figure 5.5: Plot of the calibrated function $\varphi(\theta_t)$.

Lastly, in Table 5.1 the list of of average 2-norm distances, D_i, between market and model prices in bps of the forward price for the i'th maturity are given. We see that the calibration is still reasonably good, but that the distances are of a higher order than those for European options. We can now check whether an eSSVI calibration on this data would result in greater accuracy. To do this, we need to find the eSSVI equivalent local volatility, since this is needed in the trinomial tree.

i	1	2	3	4	5	6	7	8	9	10	11
D_i	1.87	2.01	3.94	2.51	2.61	4.23	4.42	3.91	7.68	14.54	20.21

Table 5.1: Table of distances of calibrated SSVI model to the American option data per maturity.

5.5 eSSVI equivalent local volatility

Just as with SSVI, we compare the eSSVI equivalent local volatillity to determine the calibration quality. Using (5.5) the eSSVI local volatility can be written as:

$$\sigma_{loc}^2 = \frac{\frac{1}{2}\left(1 + \frac{1+\rho\varphi k}{\sqrt{\varphi^2k^2+2\rho\varphi k+1}} + k\partial_\theta(\theta\varphi)\frac{\varphi k}{\sqrt{\varphi^2k^2+2\rho\varphi k+1}} + k\partial_\theta(\theta\rho\varphi)\left(1 + \frac{1}{\sqrt{\varphi^2k^2+2\rho\varphi k+1}}\right)\right)\frac{\partial\theta}{\partial t}}{a(k) - b(k)\varphi^2\theta - \frac{c(k)}{16}\varphi^2\theta^2} \tag{5.24}$$

We examine what happens when $\theta_t \to 0$ when $k = 0$ and when $k \to \pm\infty$. For the first case we see that the value of $g(k)$ does not change, therefore it is still:

$$g(0) = \frac{\theta\varphi^2}{4} - \frac{\theta\varphi^2\rho^2}{2} - \frac{\theta^2\varphi^2\rho^2}{16} + 1, \tag{5.25}$$

resulting in the ATM local volatility:

$$\sigma_{loc}^2(k=0) = \frac{16\frac{\partial\theta}{\partial t}}{4\theta\varphi^2 - 8\theta\varphi^2\rho^2 - \theta^2\varphi^2\rho^2 + 16}. \tag{5.26}$$

This value is the same as for the SSVI equivalent local volatility, so again there is the problem that if we take our power-law form for φ that it is required that $\lambda \in [0, 1/2)$, or else the value does not go to $\frac{\partial\theta}{\partial t}$ as $\theta_t \to 0$.

For $k \to \pm\infty$, we have that:

$$\lim_{k\to\pm\infty}\sigma_{loc}^2 = \frac{64\lim_{k\to\pm\infty}\frac{\partial w}{\partial t}}{16 - \theta^2\varphi^2(1\pm\rho)^2} = \frac{32\lim_{k\to\pm\infty}\left(1 \pm \rho \pm k\varphi\gamma + k\varphi(\delta+\rho\gamma)\right)\frac{\partial\theta}{\partial t}}{16 - \theta^2\varphi^2(1\pm\rho)^2} \to \pm\infty \tag{5.27}$$

However, it is clear that the eSSVI equivalent local volatility goes to infinity in the wings at the rate $\sqrt{k}$, as $\lim_{k\to\pm\infty}\frac{\sigma_{loc}^2}{k} = \frac{\varphi(\delta+(\rho\pm\gamma))\partial_t\theta}{16-\theta^2\varphi^2(1\pm\rho)^2}$, is a constant in k.

Using this eSSVI equivalent local volatility, American option prices can be generated with the trinomial tree.

5.6 American calibration with eSSVI

We can now calibrate eSSVI on the same `ING` option data. In the case of European options, we knew the values for θ_t are identical since the same method is used to find these values in both calibrations. However, we have that θ_t is a free variable that is calibrated along with the other model parameters with the only requirement being that the values are strictly increasing in time. Strangely enough, we find that the values for θ_t for eSSVI are in fact

nearly equivalent to those found for SSVI. The same holds for the parameters η and λ, where we now derive them to be 0.866 and 0.499 respectively, compared to 0.871 and 0.496 for SSVI. Hence, the function $\varphi(\theta_t)$ is also very similar for both cases.

For ρ the following function is derived:

$$\rho(\theta_t) = 0.123 \exp(-250.0\theta_t) - 0.545 \tag{5.28}$$

This function in plotted in Figure 5.6.

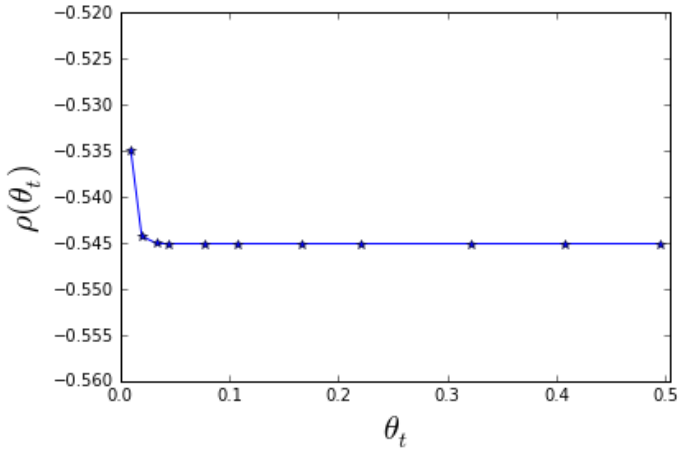

Figure 5.6: Plot of the optimal function of $\rho(\theta_t)$

In Figure 5.7 we added the calibrated constant SSVI value for ρ to compare. It is clear that there are only minor differences, even for the first couple maturities. It is thus clear that in terms of the parameters there is essentially very little difference between SSVI and eSSVI in this case.

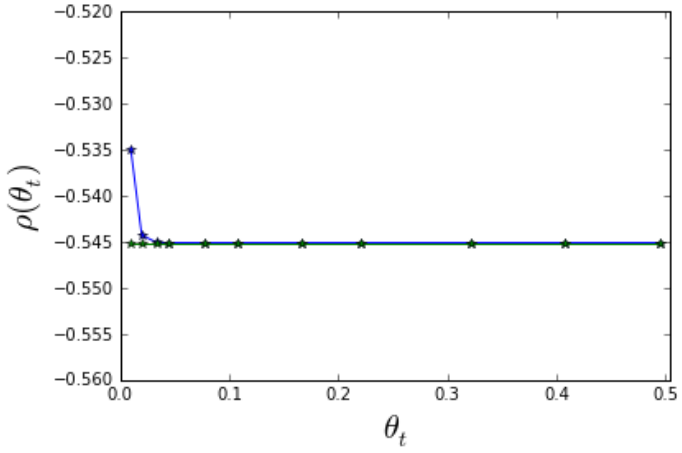

Figure 5.7: Comparison of the calibrated SSVI and eSSVI ρ on American option data

Table 5.2 lists the average distance between market and model price per maturity for eSSVI. This table shows nearly identical values as Table 5.1, which could be expected since both the values for θ_t as $\varphi(\theta_t)$ are approximately identical for the two models and $\rho(\theta_t)$ is nearly constant for the majority of the maturities listed in the market. From this particular data set we would be led to believe that, whereas eSSVI has a noticeable impact on calibration quality for European options, American options do not enjoy this increase in performance.

i	1	2	3	4	5	6	7	8	9	10	11
D_i	1.80	2.04	3.84	2.48	2.59	4.21	4.42	3.93	7.70	14.48	20.61

Table 5.2: Table of distances of calibrated eSSVI model to the American option data per maturity.

5.7 Summary

After introducing our new surface model in the previous chapter, we demonstrated how such a surface model can be transformed to a local volatility to be used in the pricing of exotic options. Using the trinomial tree with local volatility, we were able to very accurately price American option. We used this to calibrate both the SSVI and eSSVI parameters on an `ING` option data set. From this, we could see that the accuracy of our model was good but not excellent and that, at least for this particular data set, there was very little difference between the outcomes of SSVI and eSSVI. It is possible though that by using better pricing methods, like the American early exercise boundary in terms of the local volatility as described by Broadie and Detemple [3], greater model accuracy can be attained.

Chapter 6

Conclusion

In this thesis we have introduced an extension to the volatility surface model SSVI which we have called eSSVI. We explored both models vigorously and compared the quality in terms of their accuracy with respect to market data. We saw that, despite the slightly added difficulty of the model, eSSVI still performed significantly better on European market data with the added benefit that it showed little added inaccuracy in times of crisis, unlike SSVI.

We also examined at a method using local volatilities such that our volatility surfaces can be used to price exotic options through the use of a trinomial tree. This method was shown to work reasonably well for American options, however the added benefits of eSSVI over SSVI disappeared. Where other exotics or data sets might display different results, the use of eSSVI over SSVI would not wholeheartedly be endorsed in this scenario.

6.1 Future research

Naturally, there is still more than enough to be explored in this research field. Possible topics include:

- We have seen that the transformation of an implied volatility surface like SSVI requires that $\lim_{\theta \to 0} g(0) = 1$. However, this is not always the case, as was when the power-law form for $\varphi(\theta)$ had the optimal parameter $\lambda = 1/2$. As we are uncertain what to do in this scenario, this could be looked into.

- From the various calibration performed in this thesis, there is a rising suspicion that calibrating on stock options, like `ING` for instance, are much less accurate than index options like `SPX`. It is possible that, in the calibration of a volatility surface on market data, this should only really be done for indexes.

- As the data used for the calibrations was rather basic, it could be checked whether SSVI or eSSVI still perform well when the market displays more extreme implied volatility smiles.

Appendix A

Alternative choices for $\varphi(\theta)$

Thus far we have kept from using any other function for $\varphi(\theta)$ than the basic power-law form: $\varphi(\theta) = \eta\theta^{-\lambda}$. We have already seen that in order to ensure that SSVI is arbitrage-free, we require $\lambda \in [0, 1/2)$ and:

$$\begin{cases} \eta \leq \frac{2\theta_{max}^{\lambda-1/2}}{\sqrt{1+|\rho|}} & \text{if } \theta_{max} < \frac{4}{1+|\rho|}, \\ \eta \leq \frac{4\theta_{max}^{\lambda-1}}{1+|\rho|} & \text{if } \theta_{max} \geq \frac{4}{1+|\rho|}. \end{cases} \tag{A.1}$$

For eSSVI, we saw that, in addition to this, we also required:

$$\begin{cases} \left|c - \frac{a}{1-\lambda}\exp(\lambda-2)\right| \leq 1, \\ |a+c| \leq 1, \\ |c| \leq 1. \end{cases} \tag{A.2}$$

There have however been other suggestions by Gatheral and Jacquier for this function $\varphi(\theta)$, which we will test here. We will look at two in particular, namely:

$$\varphi(\theta) = \eta\theta^{-\lambda}(1+\theta)^{\lambda-1} \quad \text{and} \quad \varphi(\theta) = \frac{\eta}{\lambda\theta}\left(1 - \frac{1-\exp(-\lambda\theta)}{\lambda\theta}\right), \tag{A.3}$$

which we will call the complex power-law and the Heston-like form respectively. Using both the constant ρ in the SSVI parametrization and the exponential form: $\rho(\theta) = a\exp(-b\theta)+c$ in the eSSVI parametrization, we will look at the arbitrage-free conditions for these different choices of φ and also check the difference in model accuracy depending on this choice.

A last thing we will look at for both alternatives concerns the finding of an SSVI or eSSVI equivalent local volatility. As we have seen for the basic power-law, we encounter difficulties whenever θ tends to zero and $\lambda = 1/2$. The reason for this was that we expect $\lim_{\theta\to 0} g(0) = 1$, where:

$$g(0) = \frac{4\theta_t\varphi(\theta_t)^2 - 8\theta_t\varphi(\theta_t)^2\rho^2 - \theta_t^2\varphi(\theta_t)^2\rho^2 + 16}{16}. \tag{A.4}$$

We will thus check whether this is true for all allowed arbitrage-free surfaces under our alternative $\varphi(\theta)$ functions.

A.1 Choice of φ under a constant ρ

We start by looking at the SSVI case. From Theorem 2.5.1 and 2.5.2 we can be sure that we are free of static arbitrage for any value of ρ when: $0 \leq \gamma \leq 1$, where $\gamma := \frac{\partial_\theta(\theta\varphi)}{\varphi}$, and:

$$\begin{cases} \theta\varphi(\theta) < \frac{4}{1+|\rho|} & \text{if } \theta \geq \frac{4}{1+|\rho|} \\ \theta\varphi(\theta)^2 \leq \frac{4}{1+|\rho|} & \text{if } \theta < \frac{4}{1+|\rho|} \end{cases}. \tag{A.5}$$

We will look at these conditions for our two alternative φ parametrizations.

A.1.1 Complex power-law form

Before we start, a quick note on the origin of this parametrization. When checking the butterfly conditions of the simple power-law parametrization, we found that it would never be arbitrage-free for all values of $\theta > 0$ as the function $\theta\varphi(\theta)$ was strictly increasing. However, we dealt with this problem by stating that we only needed the model to be free of butterfly arbitrage up to the final maturity given in the market, meaning that we only needed the function to be bounded for $\theta \leq \theta_{max}$. Although this works in practice, it is not exactly mathematically sound. We would prefer it if we had a function $\varphi(\theta)$ such that we had no arbitrage for all $\theta \geq 0$. For this reason, the complex power-law form was introduced.

In order to be free of calendar spread arbitrage, we check the function γ for this form. We find that:

$$\gamma = \frac{1-\lambda}{1+\theta}, \tag{A.6}$$

meaning that from the positivity of θ that $0 \leq \gamma \leq 1$ if and only in $\lambda \in [0, 1]$. If we then look at the butterfly arbitrage conditions, we see however that:

$$\lim_{\theta\to 0} \theta\varphi(\theta)^2 = \lim_{\theta\to 0} \eta\theta^{1-2\lambda}\theta^{2\lambda-2} \to \infty, \tag{A.7}$$

when $\lambda \in (1/2, 1]$. Therefore, we again have that $\lambda \in [0, 1/2]$. We can also find that the function $\theta\varphi(\theta)$ is strictly increasing with:

$$\lim_{\theta\to\infty} \eta \left(\frac{\theta}{1+\theta}\right)^{1-\lambda} = \eta, \tag{A.8}$$

and that the function $\theta\varphi(\theta)^2$ has a maximum at $\theta = 1 - 2\lambda$. Combining this, we see that for this form with a constant ρ, we have an arbitrage-free SSVI surface if $\lambda \in [0, 1/2)$ and:

$$0 \leq \eta \leq \min\left(\frac{4}{1+|\rho|}, \frac{2(1-2\lambda)^{\lambda-1/2}(2\lambda-2)^{1-\lambda}}{1+|\rho|}\right). \tag{A.9}$$

Lastly we look at the function $g(0)$. Clearly, we have under the conditions above that: $\lim_{\theta\to 0} \theta\varphi(\theta) = 0$, and:

$$\lim_{\theta\to 0} \theta\varphi(\theta)^2 = \lim_{\theta\to 0} \eta^2\theta^{1-2\lambda}(1+\theta)^{2\lambda-2} = \begin{cases} 0 & \text{if } \lambda \in [0, 1/2), \\ \eta^2 & \text{if } \lambda = 1/2. \end{cases} \tag{A.10}$$

Therefore, we still have the same issue as we had with the basic power-law when $\lambda = 1/2$, so we will omit this case from our conditions as well.

A.1.2 Heston-like form

For the Heston-like for, we see that:

$$\gamma = \frac{1 - (1 + \lambda\theta)\exp(-\lambda\theta)}{\lambda\theta - 1 + \exp(-\lambda\theta)}, \tag{A.11}$$

which is a strictly decreasing function for $\lambda > 0$ with a limit equal to one when θ tends to zero. So we see that if indeed $\lambda > 0$ we are free of calendar spread arbitrage. Next, we can find for these values for λ that the function $\theta\varphi(\theta)$ is strictly increasing with:

$$\lim_{\theta\to\infty} \theta\varphi(\theta) = \lim_{\theta\to\infty} \frac{\eta}{\lambda^2\theta}(\lambda\theta - 1 + \exp(-\lambda\theta)) = \frac{\eta}{\lambda}, \tag{A.12}$$

meaning that we have:

$$\eta \leq \frac{4\lambda}{1 + |\rho|}. \tag{A.13}$$

We can also find that $\theta\varphi(\theta)^2$ has a maximum at θ such that: $\exp(\lambda\theta) = \frac{3+2\lambda\theta}{3-\lambda\theta}$. Since we cannot solve this for θ, we can only find an approximation of the maximum of $\theta\varphi(\theta)^2$ by using a Taylor expansion. Replacing $\exp(\lambda\theta)$ with its fourth order expansion, we can find that the maximum is located at approximately $\theta \approx 2/\lambda$, meaning that we have the bound:

$$\eta \leq \frac{1}{1 + \exp(-2)}\sqrt{\frac{32\lambda}{1 + |\rho|}}. \tag{A.14}$$

This will, however, still leave the risk that the resulting bound is not strict enough to fully prevent butterfly arbitrage.

Although this form of φ has the issue that we do not have exact bounds to prevent arbitrage, we do find that:

$$\lim_{\theta\to 0} \theta\varphi(\theta) = \lim_{\theta\to 0} \theta\varphi(\theta)^2 = 0, \tag{A.15}$$

meaning that in this case, we have no issues when converting the SSVI surface to local volatilities.

A.2 Choice of $\varphi(\theta)$ under an exponential $\rho(\theta)$

If we take the exponential form for $\rho(\theta)$, we have to use the eSSVI conditions for calendar-spread arbitrage, meaning that:

$$|\delta + \rho\gamma| \leq \gamma, \text{ where } \delta := \theta\partial_\theta(\rho). \tag{A.16}$$

For all three choices, the butterfly arbitrage conditions for λ and η are almost the same as above, except that, since we do not have a constant ρ, we simplify by substituting the ρ in the formula with $\rho_{max} := \max_{\theta>0} |\rho(\theta)|$. However, for the exponential form, we know that:

$$\max_{\theta>0} |a\exp(-b\theta) + c| = \max(|a + c|, |c|), \tag{A.17}$$

which we use from now on.

A.2.1 Second power-law

For the second power-law form, we get: $|C + \frac{1-\lambda-B\theta^2-B\theta}{1-\lambda}(A-C)\exp(-B\theta)| \leq 1$. This only has one possible extremum, namely at: $\theta = \frac{2-B+D}{2B}$, where $D := \sqrt{B^2 - 4B\lambda + 4B + 4}$. This means that we require:

$$\left| C - (A-C)\frac{D+2}{B(1-\lambda)} \exp\left(\frac{B-D-2}{2}\right) \right| \leq 1. \tag{A.18}$$

If we also look at the points $\theta = 0$ and $\theta \to \infty$, we again find that $|C| \leq 1$ and $|A| \leq 1$.

A.2.2 Heston-like

Lastly, we have the Heston-like parametrization, where we now find that $\gamma = \frac{1-(1+\lambda\theta)\exp(-\lambda\theta)}{\exp(-\lambda\theta)+\lambda\theta-1)}$, which is a function that lies on $(0, 1]$ for all $\theta \geq 0$ and $\lambda > 0$. For this reason, we can write equation (A.16) as:

$$|C - (A-C)\left(\frac{B\theta}{\gamma} + 1\right)\exp(-B\theta)| \leq 1, \tag{A.19}$$

where the extremum of the LHS lies at θ such that:

$$(B\lambda\theta - B - 2\lambda)y^2 + (2B - B\lambda^2\theta^2 + \lambda^3\theta^2 + \lambda^2\theta + 4\lambda)y - B\lambda\theta - B - \lambda^2\theta - 2\lambda = 0, \text{ where } y = \exp(\lambda\theta). \tag{A.20}$$

Since we will generally have θ close to zero, we can take the third degree Taylor expansion of $\exp(\lambda\theta)$ to find an approximation, which is: $\theta \approx \frac{\sqrt{1+\frac{8\lambda}{B}}-1}{2\lambda}$. Filling this into (A.19), we find:

$$\left| C - (A-C)\left(\frac{B}{2\lambda\gamma}\left(\sqrt{1+\frac{8\lambda}{B}} - 1\right) - 1\right)\exp\left(\frac{-B}{2\lambda}\left(\sqrt{1+\frac{8\lambda}{B}} - 1\right)\right)\right| \leq 1 \tag{A.21}$$

For $\theta = 0$ and $\theta \to \infty$, we again find that $|A| \leq 1$ and $|C| \leq 1$.

A.3 Comparing the functions

Using the arbitrage-free bounds on our parameters for the various functions of φ, we can determine which of the functions would lead to the most accurate SSVI and eSSVI surface. This is done using the `SPX` data set from 22/02/16, where we look at both the calibrated SSVI and eSSVI parameters and the resulting model error. This model error is expressed as the average 2-norm distance between the model and market prices per maturity in bps of the forward price. For SSVI, we derive a model error of 0.429 for the basic power-law, 0.380 for the complex power-law and 0.505 for the Heston-like form. This means that, compared with the basic power-law form, the complex version performs better at a rate of approximately 1.128. The Heston-like form however, performs worse at a rate of 0.849.

For eSSVI, the model errors are derived with the value 0.296 for the basic power-law, 0.255 for the complex power-law and 0.436 for the Heston-like form. Nearly the same ratios are found here, as the complex power-law performs about 1.161 times better than the basic

power-law, whereas the Heston-like form again performs worse at a ratio of 0.680.

Although we have seen that there are never problems when converting the SSVI or eSSVI implied volatility to a local volatility when one chooses the Heston-like form in the model, it clearly is an inferior choice to either power-law form in terms of model accuracy. Between these two, only a minor loss in accuracy is found when opting for the basic form over the complex form. However, due to fact that it can guarantee a fully butterfly arbitrage free surface for all $\theta > 0$, it would be advised to choose the complex form over the basic power-law form.

Appendix B

A family of functions for $\rho(\theta)$

In Section 4.3, we found the following continuous conditions for a volatility surface with the functions $\rho(\theta)$ and $\varphi(\theta)$ to be free of calendar spread arbitrage:

$$\begin{aligned} \frac{\partial\theta}{\partial t} \geq 0 \quad &\text{and} \quad -\gamma \leq \delta + \rho\gamma \leq \gamma \\ \gamma \leq 1 \quad &\text{or} \quad -\sqrt{2\gamma - 1} \leq \delta + \rho\gamma \leq \sqrt{2\gamma - 1}, \end{aligned}$$

where $\delta = \theta\frac{\partial\rho}{\partial\theta}$ and $\gamma = \frac{1}{\varphi}\frac{\partial(\theta\varphi)}{\partial\theta}$.

The power-law function $\varphi(\theta) = \eta\theta^{-\lambda}$ has also been found to work well for the model, meaning that:

$$0 \leq \frac{\partial_\theta(\theta\varphi(\theta))}{\varphi(\theta)} \leq 1. \tag{B.1}$$

Knowing this, solving the differential equation: $\delta + \rho(\theta)\gamma = u\gamma$, with u a function parameter with values in $[-1, 1]$, will give us a family of functions for ρ that fulfils the arbitrage-free conditions.

B.1 General function $\varphi(\theta)$

Looking at $|\delta + \rho\gamma| \leq \gamma$, which can be written as: $|\theta\partial_\theta(\rho(\theta)) + \rho(\theta)\partial_\theta(\theta\varphi(\theta))| \leq \frac{\partial_\theta(\theta\varphi(\theta))}{\varphi(\theta)}$. We note that:

$$\frac{\partial(\theta\varphi(\theta)\rho(\theta))}{\partial\theta} = \theta\varphi(\theta)\frac{\partial(\rho(\theta))}{\partial\theta} + \rho(\theta)\frac{\partial(\theta\varphi(\theta))}{\partial\theta}. \tag{B.2}$$

Dividing this by $\varphi(\theta)$, our condition becomes:

$$|\partial_\theta(\theta\varphi\rho)| \leq \partial_\theta(\theta\varphi). \tag{B.3}$$

It is now possible to find a function $u(\theta)$, with the condition that for all $\theta > 0 :\ u(\theta) \in [-1, 1]$, such that we can say: $\partial_\theta(\theta\varphi(\theta)\rho(\theta)) = u(\theta)\partial_\theta(\theta\varphi(\theta))$. Integrating both sides gives us, using $\theta\varphi(\theta) \to 0$ as $\theta \to 0$:

$$\theta\varphi(\theta)\rho(\theta) = \int_0^\theta u(\tau)\partial_\tau(\tau\varphi(\tau))d\tau. \tag{B.4}$$

If we now divide both sides by $\theta\varphi(\theta)$ and perform the change of variable: $\tau = r\theta$, with $r \in [0,1]$, we now get:

$$\rho(\theta) = \frac{1}{\varphi(\theta)} \int_0^1 u(r\theta)\partial_r(r\varphi(r\theta))dr \tag{B.5}$$

From this we see that for a given function $\varphi(\theta)$, by choosing a valid function for $u(\theta)$ such that for all $\theta > 0$: $\left|\frac{1}{\varphi(\theta)} \int_0^1 u(r\theta)\partial_r(r\varphi(r\theta))dr\right| \leq 1$, we get an admissible $\rho(\theta)$.

From (B.5) and the fact that we can write $u(\theta) = \frac{\partial_\theta(\theta\varphi(\theta)\rho(\theta))}{\partial_\theta(\theta\varphi(\theta))}$, we can either choose a function for $\rho(\theta)$ and check whether the resulting function $u(\theta)$ lies in $[-1,1]$, or choose such a function $u(\theta)$ and solve to find $\rho(\theta)$. Note that it might be possible for the function $\rho(\theta)$ from (B.5) to allow values outside of $(-1,1)$. However, if we define: $u^*(\theta) = \sup_{r\in[0,1]} |u(r\theta)|$ and remember that we define $\varphi(\theta)$ such that: $0 \leq \frac{\partial_\theta(\theta\varphi(\theta))}{\varphi(\theta)} \leq 1$, we can write this as:

$$\begin{aligned}
\left|\frac{1}{\varphi(\theta)} \int_0^1 u(r\theta)\partial_r(r\varphi(r\theta))dr\right| &\leq \frac{1}{\varphi(\theta)} \int_0^1 |u(r\theta)|\partial_r(r\varphi(r\theta))dr && \text{(B.6)}\\
&\leq \frac{u^*(\theta)}{\varphi(\theta)} \int_0^1 \partial_r(r\varphi(r\theta))dr && \text{(B.7)}\\
&= u^*(\theta)\frac{[r\varphi(r\theta)]_0^1}{\varphi(\theta)} && \text{(B.8)}\\
&= u^*(\theta) && \text{(B.9)}
\end{aligned}$$

From the definition of $u(\theta)$, we know that $u^*(\theta) \leq 1$, and therefore we see that $\rho(\theta) \in (-1,1)$ always holds.

B.1.1 Simple power-law

Here we look at the case when we choose the function $\varphi(\theta) = \eta\theta^{-\lambda}$. Here we get:

$$\begin{aligned}
\rho(\theta) &= \frac{1}{\eta\theta^{-\lambda}} \int_0^1 u(r\theta)\partial_r(r\eta(r\theta)^{-\lambda})dr\\
&= (1-\lambda)\int_0^1 u(r\theta)r^{-\lambda}dr.
\end{aligned}$$

Choosing any function $u(\theta) \in [-1,1]$ will now result in a function $\rho(\theta)$ such that the surface is free of calendar spread arbitrage.

Example

If we were now willing to find the function $u(\theta)$ corresponding to the function $\rho(\theta) = a\exp(-b\theta) + c$, we have that: $u(\theta) = \frac{\partial_\theta(\theta\varphi(\theta)\rho(\theta))}{\partial_\theta(\theta\varphi(\theta))}$, so:

$$\begin{aligned}
u(\theta) &= \frac{\partial_\theta(\eta\theta^{-\lambda}(a\exp(-b\theta) + c))}{\partial_\theta(\eta\theta^{-\lambda})}\\
&= c + \frac{1-\lambda-\theta b}{1-\lambda} a\exp(-b\theta).
\end{aligned}$$

This is the exact same condition as we had in Section 4.4, where we saw that $u(\theta) \in [-1, 1]$ if and only if:

$$\begin{cases} |c - \frac{a}{1-\lambda} \exp(\lambda - 2)| \leq 1, \\ |a + c| \leq 1, \\ |c| \leq 1. \end{cases} \tag{B.10}$$

Bibliography

[1] F. Black, M. Scholes (1973): *The Pricing of Options and Corporate Liabilities,* The Journal of Political Economy, No. 81, 637-654.

[2] P.T. Boggs, J.W. Tolle (1995): *Sequential quadratic programming*, Acta numerica 4, 1-51.

[3] M. Broadie, J. Detemple (1996): *American Options on Dividend-Paying Assets*, Scientific Series, 96s-15.

[4] P. Carr, D.B. Madan (2005): *A note on sufficient conditions for no arbitrage,* Finance Research Letters 2, 125-130.

[5] E. Derman, I. Kani, J.Z. Zou (1996): *The Local Volatility Surface: Unlocking the Information in Index Option Prices*, Financial Analysts Journal, Vol. 52, No 4.

[6] B. Dupire (1994): *Pricing with a smile*, Risk 7, 18-20.

[7] P. Dybvig, S. Ross (1987): *Arbitrage*, The New Palgrave: A Dictionary of Economics 1, 100-106.

[8] F.N. Fritsch, R.E. Carlson (1980): *Monotone Piecewise Cubic Interpolation*, SIAM Journal on Numerical Analysis, 17 (2), 238246.

[9] J. Gatheral (2004): *A parsimonious arbitrage-free implied volatility parameterization with application to the valuation of volatility derivatives*, Presentation at Global Derivatives.

[10] J. Gatheral (2006): *The Volatility Surface, A Practitioner's Guide*, Wiley Finance.

[11] J. Gatheral, A. Jacquier (2013): *Arbitrage-free SVI volatility surfaces,* Quantitative Finance, Vol. 14, No. 1, 59-71.

[12] G. Guo, A. Jacquier, C. Martini, L. Neufcourt (2012): *Generalised Arbitrage-free SVI Volatility Surfaces.*

[13] P.S. Hagan, D. Kumar, A. Lesniewski, D.E. Woodward (2002): *Managing Smile Risk* Wilmott Magazine, 84-108.

[14] J. Hull (2006): *Options, Futures, and Other Derivatives.* Upper Saddle River, N.J: Pearson/Prentice Hall.

[15] R. Lee (2004): *The moment formula for implied volatility at extreme strikes*, Mathematical Finance 14(3), 469-480.

[16] P. Wilmott, S. Howison, J. Dewynne (1995): *The Mathematics of Financial Derivatives*, Cambridge University Press.